Skew-symmetric entropy stable discontinuous Galerkin formulations with applications to hybrid meshes

Jesse Chan

Abstract Entropy stable high order methods for nonlinear conservation laws satisfy an inherent discrete entropy inequality. The construction of such schemes has relied on the use of carefully chosen collocation points [1–5] or volume and surface quadrature rules [6, 7] to produce operators which satisfy a summation-by-parts (SBP) property. In this work, we show how to construct skew-symmetric schemes which are entropy stable even for volume and surface quadratures under which a traditional SBP property does not hold. These skew-symmetric formulations avoid the use of a "strong" SBP property, and require only that operators exactly differentiate constants and satisfy a discrete form of the fundamental theorem of calculus. We conclude with an application of the skew-symmetric formulation for entropy stable schemes on mixed quadrilateral-triangle meshes.

Contents

J. Chan
Department of Computational and Applied Mathematics
Rice University
6100 Main Street
Houston, TX, 77005
E-mail: jesse.chan@rice.edu

1 Introduction

High order methods for the simulation of time-dependent compressible flow have the potential to achieve higher levels of accuracy at lower costs compared to current low order schemes [8]. In addition to superior accuracy, the low numerical dispersion and dissipation of high order methods [9] enables the accurate propagation of waves over long distances and time scales. The same properties also make high order methods attractive for unsteady phenomena such as vorticular and turbulent flows, which are sensitive to numerical dissipation [8, 10].

However, when applied to nonlinear conservation laws, high order methods can experience artificial growth and blow-up near under-resolved features such as shocks or turbulence. In practice, the application of high order methods to practical problems requires shock capturing and stabilization techniques (such as artificial viscosity) or solution regularization (such as filtering or limiting) to prevent solution blow-up. The resulting schemes for nonlinear conservation laws walk a fine line between stability, robustness, and accuracy. Aggressive stabilization or regularization can result in the loss of high order accuracy, while too little can result in instability [8]. Moreover, it can be difficult to determine robust expressions for stabilization paramaters, as parameters which work for one simulation can fail when applied to a different physical regime or discretization setting.

These issues have motivated the introduction of high order *entropy stable* discretizations, which satisfy a semi-discrete entropy inequality while maintaining high order accuracy in smooth regions. Proofs of continuous entropy inequalities rely on the chain rule, which does not hold discretely due to effects such as quadrature error. By using an approach referred to as "flux differencing", entropy stable schemes account for the loss of the chain rule while maintaining a semi-discrete analogue of the continuous entropy inequality. These schemes were first introduced as high order collocation methods on tensor product elements in [2, 3, 11, 12], and were extended to simplicial elements in [4, 6, 7, 13, 14]. Entropy stable methods have also been extended to a variety of other discretization settings, including staggered grids [15], Gauss-Legendre collocation [5], and non-conforming meshes [16].

Entropy stable discretizations are built upon flux differencing and a summation-by-parts (SBP) property, which serves as a discrete analogue of integration by parts for quadrature-based discretization matrices. However, the SBP property does not hold for some under-integrated quadrature rules, which naturally arise in certain discretization settings. For example, on hybrid meshes consisting of both quadrilateral and triangular elements, it is convenient to utilize the same quadrature rule on shared faces between different element types. On degree N tensor product elements, a popular choice of quadrature is an $(N + 1)$-point Gauss-Legendre-Lobatto (GLL) rule. When both volume and surface integrals are approximated using $(N + 1)$ point GLL quadrature rules, the SBP property holds, despite the fact that GLL quadrature is inexact for the integrands which appear in finite element formulations [2]. However, while GLL quadrature induces an SBP property on quadrilateral elements, but does not always result in an SBP property if used for triangular elements [6].

This work proposes an alternative formulation which utilizes a skew-symmetric form of flux differencing. Under such a formulation, the proof of entropy stability requires only a weaker "variational" form of the SBP property, which holds under a more general class of quadrature rules compared to the decoupled SBP property

introduced in [6, 7]. We show that the skew-symmetric formulation is entropy stable, locally conservative, and free-stream preserving on curved elements, and confirm theoretical results with numerical experiments on triangular, quadrilateral, and hybrid triangular-quadrilateral meshes.

It should be noted that a similar approach to entropy stable discretizations was introduced within a finite difference framework [4, 14] using multidimensional differencing operators which are constructed to satisfy accuracy conditions and an SBP property [17]. These operators do not correspond to any specific basis or approximation space, but can be shown to exist for nodal points corresponding to sufficiently accurate choices of volume and surface quadrature and can be computed either algebraically or through an optimization problem. The formulations presented in this work require similar accuracy conditions, but differ from those of [4, 14] in that we start with an explicit approximation space, which then induce quadrature-based operators. The formulations presented here also accomodate general choices of volume and surface quadrature (e.g. volume quadratures without boundary nodes and over-integrated rules) while ensuring compact coupling conditions between neighboring elements.

The structure of the paper is as follows: Section 2 describes the continuous entropy inequality which we aim to replicate discretely. Section 3 and Section 4 introduce polynomial approximation spaces and quadrature-based SBP operators on simplicial and tensor product elements. Section 5 then introduces the variational SBP property and an entropy conservative skew-symmetric formulation. Section 6 extends the skew-symmetric formulation to curved elements, and Section 8 presents numerical experiments which verify the theoretical assumptions, stability, and accuracy of the proposed formulations.

2 Entropy stability for systems of nonlinear conservation laws

We begin by reviewing the dissipation of entropy for a d-dimensional system of nonlinear conservation laws on a domain Ω

$$\frac{\partial \boldsymbol{u}_h}{\partial t} + \sum_{j=1}^{d} \frac{\partial \boldsymbol{f}_j(\boldsymbol{u})}{\partial x_j} = 0, \qquad \boldsymbol{u} \in \mathbb{R}^n, \qquad \boldsymbol{f} : \mathbb{R}^n \to \mathbb{R}^n, \tag{1}$$

where $\boldsymbol{u}$ are the conservative variables and $\boldsymbol{f}(\boldsymbol{u})$ is a vector-valued nonlinear flux function. We are interested in nonlinear conservation laws for which a convex entropy function $U(\boldsymbol{u})$ exists. For such systems, the *entropy variables* are an invertible mapping $\boldsymbol{v}(\boldsymbol{u}) : \mathbb{R}^n \to \mathbb{R}^n$ defined as the derivative of the entropy function with respect to the conservative variables

$$\boldsymbol{v}(\boldsymbol{u}) = \frac{\partial U}{\partial \boldsymbol{u}}. \tag{2}$$

Several widely used equations in fluid modeling (Burgers, shallow water, compressible Euler and Navier-Stokes equations) yield convex entropy functions $U(\boldsymbol{u})$ [14, 18]. Let $\partial\Omega$ be the boundary of Ω with outward unit normal $\boldsymbol{n}$. By multiplying the equation (1) with $\boldsymbol{v}(\boldsymbol{u})^T$, the solutions $\boldsymbol{u}$ of (1) can be shown to satisfy an

entropy inequality

$$\int_{\Omega} \frac{\partial U(\boldsymbol{u})}{\partial t} \, \mathrm{d}x + \int_{\partial\Omega} \sum_{j=1}^{d} \left(\boldsymbol{v}(\boldsymbol{u})^T \boldsymbol{f}_j(\boldsymbol{u}) - \psi_j\left(\boldsymbol{v}(\boldsymbol{u})\right) \right) n_j \, \mathrm{d}x \leq 0, \qquad (3)$$

where $\boldsymbol{n} = (n_1, \ldots, n_d)$ denotes the outward unit normal, and $\psi_j(\boldsymbol{u})$ is some function referred to as the entropy potential.

The proof of (3) requires the use of the chain rule [19–21]. The instability-in-practice of high order schemes for (1) can be attributed in part to the fact that the discrete form of the equations do not satisfy the chain rule, and thus do not satisfy (3). As a result, discretizations of (1) do not typically possess an underlying statement of stability. For low order schemes, this can be offset in practice by the inherent numerical dissipation. However, because high order discretizations possess low numerical dissipation, the lack of an underlying discrete stability has been conflated with the idea that high order methods are inherently less stable than low order methods.

3 Polynomial approximation spaces

In this work, we consider either simplicial reference elements (triangles and tetrahedra) or tensor product reference elements (quadrilaterals and hexahedra). We define an approximation space using degree N polynomials on the reference element; however, the natural polynomial approximation space differs depending on the element type [22].

On a d-dimensional reference simplex, the natural polynomial space are total degree N polynomials

$$P^N\left(\widehat{D}\right) = \left\{ \widehat{x}_1^{i_1} \ldots \widehat{x}_d^{i_d}, \quad \widehat{\boldsymbol{x}} \in \widehat{D}, \quad 0 \leq \sum_{k=1}^{d} i_k \leq N \right\}.$$

In contrast, the natural polynomial space on a d-dimensional tensor product element is the space of maximum degree N polynomials

$$Q^N\left(\widehat{D}\right) = \left\{ \widehat{x}_1^{i_1} \ldots \widehat{x}_d^{i_d}, \quad \widehat{\boldsymbol{x}} \in \widehat{D}, \quad 0 \leq i_k \leq N, \quad k = 1, \ldots, d \right\}.$$

We denote the natural approximation space on a given reference element $\widehat{D}$ by V^N. Furthermore, we denote the dimension of V^N as $N_p = \dim\left(V^N\left(\widehat{D}\right)\right)$.

The proofs presented in this work will also use anisotropic tensor product polynomial spaces, where the maximum polynomial degree varies depending on the coordinate direction. We denote such spaces by $Q^{N_1, \ldots, N_d}$, where N_k are non-negative integers and

$$Q^{N_1, N_2, \ldots, N_d}\left(\widehat{D}\right) = \left\{ \widehat{x}_1^{i_1} \ldots \widehat{x}_d^{i_d}, \quad \widehat{\boldsymbol{x}} \in \widehat{D}, \quad 0 \leq i_k \leq N_k, \quad k = 1, \ldots, d \right\}.$$

For example, the isotropic tensor product space Q^N is the same as $Q^{N, \ldots, N}$.

We also define trace spaces for each reference element. Let $\widehat{f}$ be a face of the reference element $\widehat{D}$. The trace space $V^N\left(\widehat{f}\right)$ is defined as the restrictions

of functions in $V^N\left(\widehat{D}\right)$ to $\widehat{f}$, and denote the dimension of the trace space as $\dim\left(V^N\left(\widehat{f}\right)\right) = N_p^f$.

$$V^N\left(\widehat{f}\right) = \left\{u|_{\widehat{f}}, \quad u \in V^N\left(\widehat{D}\right), \quad \widehat{f} \in \partial\widehat{D}\right\}.$$

For example, on a d-dimensional simplex, $V^N\left(\partial\widehat{D}\right)$ consists of total degree N polynomials on simplices of dimension $(d-1)$. On a d-dimensional tensor product element, $V^N\left(\partial\widehat{D}\right)$ consists of maximum degree N polynomials on a tensor product element of dimension $(d-1)$.

4 Quadrature-based matrices and decoupled SBP operators

Let $\widehat{D} \subset \mathbb{R}^d$ denote a reference element with surface $\partial\widehat{D}$. The high order schemes in [6, 7] begin by approximating the solution in a degree N polynomial basis $\left\{\phi_j(\boldsymbol{x})\right\}_{i=1}^{N_p}$ on $\widehat{D}$. These schemes also assume volume and surface quadrature rules $(\boldsymbol{x}_i, w_i), \left(\boldsymbol{x}_i^f, w_i^f\right)$ on $\widehat{D}$. We will specify the accuracy of each quadrature rule later, and discuss how quadrature accuracy implies specific summation-by-parts properties.

Let $\boldsymbol{V}_q, \boldsymbol{V}_f$ denote interpolation matrices, and let $\boldsymbol{D}^i$ be the differentiation matrix with respect to the ith coordinate such that

$$\left(\boldsymbol{V}_q\right)_{ij} = \phi_j(\boldsymbol{x}_i), \qquad \left(\boldsymbol{V}_f\right)_{ij} = \phi_j(\boldsymbol{x}_i^f), \qquad \frac{\partial\phi_j(\boldsymbol{x})}{\partial x_i} = \sum_{k=1}^{N_p} \left(\boldsymbol{D}_{jk}^i\right)\phi_k(\boldsymbol{x}). \qquad (4)$$

The interpolation matrices $\boldsymbol{V}_q, \boldsymbol{V}_f$ map basis coefficients to evaluations at volume and surface quadrature points respectively, while the differentiation matrix $\boldsymbol{D}_i$ maps basis coefficients of a function to the basis coefficients of its derivative with respect to x_k. The interpolation matrices are used to assemble the mass matrix $\boldsymbol{M}$, the quadrature-based projection matrix $\boldsymbol{P}_q$, and lifting matrix $\boldsymbol{L}_f$

$$\boldsymbol{M} = \boldsymbol{V}_q^T\boldsymbol{W}\boldsymbol{V}_q, \qquad \boldsymbol{P}_q = \boldsymbol{M}^{-1}\boldsymbol{V}_q^T\boldsymbol{W}, \qquad \boldsymbol{L}_f = \boldsymbol{M}^{-1}\boldsymbol{V}_f^T\boldsymbol{W}_f, \qquad (5)$$

where $\boldsymbol{W}, \boldsymbol{W}_f$ are diagonal matrices of volume and surface quadrature weights, respectively. The matrix $\boldsymbol{P}_q$ is a quadrature-based discretization of the L^2 projection operator Π_N onto degree N polynomials, which is given as follows: find $\Pi_N u \in V^N$ such that

$$\int_{\widehat{D}} \Pi_N uv = \int_{\widehat{D}} uv, \qquad \forall v \in V^N. \qquad (6)$$

Interpolation, differentiation, and L^2 projection matrices can be combined to construct finite difference operators. For example, the matrix $\boldsymbol{D}_q^i = \boldsymbol{V}_q\boldsymbol{D}^i\boldsymbol{P}_q$ maps function values at quadrature points to approximate values of the derivative at quadrature points. By choosing specific quadrature rules, $\boldsymbol{D}_q^i$ recovers high order summation-by-parts finite difference operators in [1, 23, 24] and certain operators in [17]. However, to address difficulties in designing efficient entropy stable interface terms for nonlinear conservation laws, a new "decoupled" summation by

parts matrix was introduced in [6] which builds interface terms directly into the approximation of the derivative.

Let $\widehat{\boldsymbol{n}}$ denote the scaled outward normal vector $\widehat{\boldsymbol{n}} = \left\{ \widehat{n}_1 \widehat{J}_f, \ldots, \widehat{n}_d \widehat{J}_f \right\}$, where $\widehat{J}_f$ is the determinant of the Jacobian of the mapping of a face of $\partial \widehat{D}$ to a reference face. Let $\widehat{\boldsymbol{n}}_i$ denote the vector containing values of the ith component $\widehat{n}_i \widehat{J} f$ at all surface quadrature points, and let $\boldsymbol{Q}^i = \boldsymbol{W} \boldsymbol{D}_q^i = \boldsymbol{W} \boldsymbol{V}_q \boldsymbol{D}^i \boldsymbol{P}_q$. The "decoupled" summation by parts operator $\boldsymbol{D}_N^i$ is defined as the block matrix involving both volume and surface quadratures

$$\boldsymbol{D}_N^i = \boldsymbol{W}_N^{-1} \boldsymbol{Q}_N^i, \qquad \boldsymbol{W}_N = \begin{pmatrix} \boldsymbol{W} & \\ & \boldsymbol{W}_f \end{pmatrix}, \qquad (7)$$

$$\boldsymbol{E} = \boldsymbol{V}_f \boldsymbol{P}_q, \qquad \boldsymbol{B}^i = \boldsymbol{W}_f \mathrm{diag}\left(\widehat{\boldsymbol{n}}_i \right), \qquad \boldsymbol{Q}_N^i = \begin{bmatrix} \boldsymbol{Q}^i - \frac{1}{2} \boldsymbol{E}^T \boldsymbol{B}^i \boldsymbol{E} & \frac{1}{2} \boldsymbol{E}^T \boldsymbol{B}^i \\ -\frac{1}{2} \boldsymbol{B}^i \boldsymbol{E} & \frac{1}{2} \boldsymbol{B}^i \end{bmatrix}.$$

Here, $\boldsymbol{B}^i$ is a boundary "integration" matrix, and $\boldsymbol{E}$ denotes the extrapolation matrix which maps values at volume quadrature points to values at surface quadrature points using quadrature-based L^2 projection and polynomial interpolation.

It was shown in [5,6] that, when combined with projection and lifting matrices, $\boldsymbol{D}_N^i$ produces a high order polynomial approximation of $f \frac{\partial g}{\partial x_i}$. Let f, g be differentiable functions, and let $\boldsymbol{f}_i = f(\boldsymbol{x}_i)$, $\boldsymbol{g}_i = g(\boldsymbol{x}_i)$ denote values of f, g at volume and surface quadrature points. Then,

$$f \frac{\partial g}{\partial x_i} \approx \begin{bmatrix} \boldsymbol{P}_q & \boldsymbol{L}_f \end{bmatrix} \mathrm{diag}\left(\boldsymbol{f} \right) \boldsymbol{D}_N^i \boldsymbol{g}. \qquad (8)$$

For sufficiently accurate quadrature rules, the matrix $\boldsymbol{Q}_N^i$ also satisfies a decoupled summation-by-parts (SBP) property, which is used to prove semi-discrete entropy stability for nonlinear conservation laws.

Theorem 1 *Assume that $\boldsymbol{Q}^i$ satisfies a generalized SBP property*

$$\boldsymbol{Q}^i = \boldsymbol{E}^T \boldsymbol{B}^i \boldsymbol{E} - \left(\boldsymbol{Q}^i \right)^T.$$

Then, the decoupled SBP operator $\boldsymbol{D}_N^i$ (7) satisfies a summation by parts property:

$$\boldsymbol{Q}_N^i + \left(\boldsymbol{Q}_N^i \right)^T = \boldsymbol{B}_N^i, \qquad \boldsymbol{B}_N^i = \begin{pmatrix} \boldsymbol{0} & \\ & \boldsymbol{B}^i \end{pmatrix}. \qquad (9)$$

Proof The proof is a straightforward extension of Theorem 1 in [6] to polynomial approximation spaces on non-simplicial elements.

The matrix $\boldsymbol{Q}^i$ satisfies a generalized SBP property if the volume and surface quadrature rules are sufficiently accurate such that the quantities

$$\int_{\widehat{D}} \frac{\partial u}{\partial \widehat{x}_j} v, \qquad \int_{\partial \widehat{D}} u v \widehat{n}_j$$

are integrated exactly for all $u, v \in V^N \left(\widehat{D} \right)$ and $j = 1, \ldots, d$. This implies that Theorem 1 is satisfied for sufficiently accurate volume and surface quadratures.

For example, on simplicial elements, (9) holds if the volume quadrature is exact for polynomial integrands of total degree $(2N - 1)$, and the surface integral is exact for degree $2N$ polynomials on each face. Tensor product elements require stricter conditions: (9) holds if both the volume and surface quadratures are exact for polynomial integrands of degree $2N$ in each coordinate, due to the fact that derivatives of $u \in Q^N$ are degree $(N-1)$ polynomials with respect to one coordinate and degree N with respect to others.

Remark 1 It should be stressed that sufficiently accurate volume and surface quadratures are not necessary conditions for Theorem 1. For example, it is well known that the use of $(N+1)$ point Gauss-Legendre-Lobatto (GLL) rules for both volume and surface quadratures result in a generalized SBP property, despite the fact that these rules are only accurate for degree $(2N - 1)$ polynomials.

When a generalized SBP property holds for $\boldsymbol{Q}^i$, entropy stability can be proven using the strong SBP property in Theorem 1 [6, 7]. The focus of this work is to address cases where the generalized SBP property (and as a result, the SBP property in Theorem 1) do not hold.

5 Skew-symmetric entropy conservative formulations on a single element

While the SBP property has been used to derive entropy stable schemes, the strong SBP property (9) is difficult to enforce in certain discretization settings, such as hybrid and non-conforming meshes. This difficulty is a result of the choices of volume and surface quadrature which naturally arise in these settings. We first illustrate how specific pairings of volume and surface quadratures can result in the loss of the SBP property (9). We then propose a skew-symmetric formulation which is entropy conservative without explicitly requiring operators which satisfy the SBP property.

5.1 Loss of the SBP property

In this section, we give examples of specific pairings of volume and surface quadratures under which the decoupled SBP property does not hold (see Figure 1). We consider two dimensional reference elements $\widehat{D}$ with spatial coordinates x, y.

Quadrilateral elements (Figure 1a) We first consider a quadrilateral element $\widehat{D}$ with an $(N+1)$ point tensor product GLL volume quadrature and $(N+1)$ point Gauss quadrature on each face. Let $u, v \in Q^N$ denote two arbitrary degree N polynomials. The assumptions of Theorem 1 are that the volume quadrature exactly integrates $\int_{\widehat{D}} \frac{\partial u}{\partial x_j} v$ and that the surface quadrature exactly integrates $\int_{\partial \widehat{D}} uv \widehat{n}_j$ on $\widehat{D}$. Because the $(N + 1)$-point Gauss rule is exact for polynomials of degree $2N + 1$ and the product $uv \in P^{2N}$ on each face, the surface quadrature satisfies the assumptions of Theorem 1. However, the 1D GLL rule is only exact for polynomials of degree $(2N - 1)$. The derivative $\frac{\partial u}{\partial x}$ is a polynomial of degree $(N - 1)$ in x, but is degree N in y. Thus, $\frac{\partial u}{\partial x} v$ is a polynomial of degree $(2N - 1)$ in x but degree $2N$ in y, and is not integrated exactly by the volume quadrature.

(a) GLL volume quadrature, Gauss
surface quadrature

(b) Degree $2N$ volume quadrature,
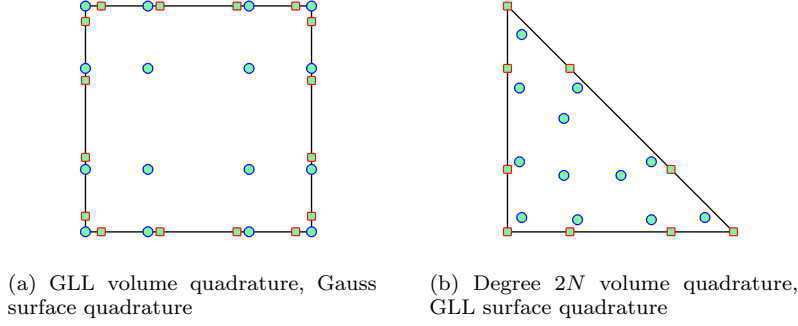GLL surface quadrature

Fig. 1: Volume and surface quadrature pairs which do not satisfy the assumptions
of Theorem 1, and thus do not possess the decoupled SBP property (9). Volume
quadrature nodes are drawn as circles, while surface quadrature nodes are drawn
as squares.

(a)   Insufficiently   accurate   surface
quadrature on the triangle element.

(b) Incompatible surface quadrature on
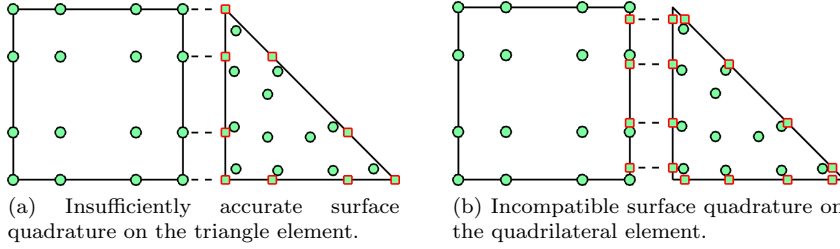the quadrilateral element.

Fig. 2: Examples of interface couplings which do not result in a decoupled SBP
property (9). Volume quadrature nodes are drawn as circles, while surface quadra-
ture nodes are drawn as squares.

Triangular elements (Figure 1b) We next consider a triangular element $\widehat{D}$, where
the volume quadrature is exact for degree $2N$ polynomials [25] and an $(N + 1)$-
point GLL quadrature on each face. Let $u, v \in P^N$ denote two arbitrary degree
N polynomials. The derivative $\frac{\partial u}{\partial x} \in P^{(N-1)}$, and $\frac{\partial u}{\partial x}v \in P^{(2N-1)}$, so the volume
quadrature satisfies the assumptions of Theorem 1. However, because the surface
quadrature is exact only degree $(2N - 1)$ polynomials and the trace of $uv \in P^{2N}$,
the surface quadrature does not satisfy the assumptions of Theorem 1.

These specific pairings of volume and surface quadratures appear naturally for
hybrid meshes consisting of DG-SEM quadrilateral elements (using GLL volume
quadrature) and triangular elements, as shown in Figure 2. In Figure 2a, the
surface quadrature is a $(N + 1)$ point GLL rule, and results in a loss of the SBP
property on the triangle. In Figure 2b, the surface quadrature is a $(N + 1)$ point
Gauss-Legendre rule, and results in a loss of the SBP property on the quadrilateral
element. The goal of this work is to construct high order accurate discretizations
which preserve entropy conservation for situations in which the decoupled SBP
property (9) does not hold.

5.2 A variational SBP property

The property (9) (which we will refer to as the "strong" SBP property) relates the polynomial exactness of specific quadrature rules to algebraic properties of quadrature-based matrices. We will relax accuracy conditions on these quadrature rules by utilizing a weaker "variational" version of the SBP property variational, which relies on the exactness of volume and surface quadrature rules only for specific polynomials.

On tensor product elements, we restrict ourselves to isotropic volume quadrature rules which are construced from tensor products of one-dimensional quadrature formulas. For the remainder of this work, the degree of the multi-dimensional quadrature rule on tensor product elements will refer to the degree of exactness of the one-dimensional rule. For example, we refer to the quadrature rule constructed through a tensor product of one-dimensional $(N + 1)$-point GLL quadrature rules as a degree $(2N - 1)$ quadrature rule. This choice of quadrature is sufficient to guarantee that the mass matrix is positive definite [26].

Throughout the remainder of this work, we make the following assumptions:

Assumption 1 *Let $v \in V^N$ denote some fixed polynomial. We assume that:*

1. *the mass matrix $\boldsymbol{M}$ is positive definite under the volume quadrature rule,*
2. *the volume quadrature rule is exact for integrals of the form*
   $\int_{\widehat{D}} \frac{\partial u}{\partial \widehat{x}_j} v$ *for all $u \in V^N\left(\widehat{D}\right)$, $j = 1, \ldots, d$.*
3. *the surface quadrature rule is exact for integrals of the form*
   $\int_{\partial \widehat{D}} u v \widehat{n}_j$ *for all $u \in V^N\left(\widehat{D}\right)$, $j = 1, \ldots, d$, and $f \in \partial \widehat{D}$.*

The conditions of Assumption 1 are relatively standard within the SBP literature [4,6,17], though they have not previously depended on the specific choice of polynomial $v(\boldsymbol{x})$. The strong SBP property (9) can be derived if Assumption 1 is satisfied for all $v \in V^N$. In contrast, we will derive a weaker SBP property which assumes only that Assumption 1 holds for a few specific polynomials v. In Sections 5.3 and 6.1, specific polynomials v will be motivated by proofs of entropy stability, and we will present examples of volume and surface quadrature rules on simplicial and tensor product elements which satisfy Assumption 1 for these choices of v.

The conditions of Assumption 1 imply the following variational SBP property:

Lemma 1 *Suppose Assumption 1 holds for $v(\boldsymbol{x}) \in V^N$, and let $\boldsymbol{v}_q$ denote the vector of values of $v(\boldsymbol{x})$ of at volume quadrature points. Let $u(\boldsymbol{x})$ be an L^2 integrable function, and let $\boldsymbol{u}_q$ denote the values of $u(\boldsymbol{x})$ at quadrature points. Then,*

$$\boldsymbol{v}_q^T \boldsymbol{Q}_i \boldsymbol{u}_q = \boldsymbol{v}_q^T \left(\boldsymbol{E}^T \boldsymbol{B}^i \boldsymbol{E} - \boldsymbol{Q}_i^T\right) \boldsymbol{u}_q.$$

Proof Recall that $\boldsymbol{Q}_i = \boldsymbol{W} \boldsymbol{V}_q \boldsymbol{D}^i \boldsymbol{P}_q$. The quadrature-based L^2 projection $\Pi_N u$ is a polynomial of degree N, and is computed discretely as $\boldsymbol{P}_q \boldsymbol{u}_q$. By the exactness of the volume quadrature in Assumption 1,

$$\boldsymbol{v}_q^T \boldsymbol{Q}_i \boldsymbol{u}_q = \boldsymbol{v}_q^T \boldsymbol{W} \boldsymbol{D}^i \boldsymbol{P}_q \boldsymbol{u}_q = \int_{\widehat{D}} \frac{\partial \Pi_N u}{\partial \widehat{x}_i} v = \int_{\partial \widehat{D}} (\Pi_N u) v \widehat{n}_i - \int_{\widehat{D}} (\Pi_N u) \frac{\partial v}{\partial \widehat{x}_i}.$$

By the exactness of the surface quadrature in Assumption 1,

$$
\int_{\partial\widehat{D}}(\Pi_N u)v\widehat{n}_i - \int_{\widehat{D}}(\Pi_N u)\frac{\partial v}{\partial \widehat{x}_i} = \boldsymbol{v}_f^T \boldsymbol{B}^i \boldsymbol{E}\boldsymbol{u}_q - \left(\boldsymbol{V}_q \boldsymbol{D}^i \boldsymbol{P}_q \boldsymbol{v}_q\right)^T \boldsymbol{W}\boldsymbol{V}_q \boldsymbol{P}_q \boldsymbol{u}_q
$$

$$
= \boldsymbol{v}_q^T \boldsymbol{E}^T \boldsymbol{B}^i \boldsymbol{E}\boldsymbol{u}_q - \boldsymbol{v}_q^T \boldsymbol{P}_q^T \left(\boldsymbol{D}^i\right)^T \boldsymbol{V}_q^T \boldsymbol{W}\boldsymbol{V}_q \boldsymbol{P}_q \boldsymbol{u}_q,
$$

where we have used that, since $v \in V^N$, $\boldsymbol{v}_f = \boldsymbol{V}_f \boldsymbol{P}_q \boldsymbol{v}_q = \boldsymbol{E}\boldsymbol{v}_q$. The proof is completed by noting that

$$
\boldsymbol{P}_q^T \left(\boldsymbol{D}^i\right)^T \boldsymbol{V}_q^T \boldsymbol{W}\boldsymbol{V}_q \boldsymbol{P}_q = \boldsymbol{P}_q^T \left(\boldsymbol{D}^i\right)^T \boldsymbol{M}\boldsymbol{P}_q = \boldsymbol{P}_q^T \left(\boldsymbol{D}^i\right)^T \boldsymbol{V}_q^T \boldsymbol{W} = \boldsymbol{Q}_i^T.
$$

The variational SBP property in Lemma 1 can be used to prove a similar property for the decoupled SBP operator. This property, along with the exact differentiation of constants, is necessary for the proof of entropy stability.

Lemma 2 *Suppose Assumption 1 holds. Let $\boldsymbol{D}_N^i$ be a decoupled SBP operator on the reference element $\widehat{D}$. Then, the following variational SBP property holds:*

$$
\boldsymbol{v}^T \boldsymbol{Q}_N^i \boldsymbol{u} = \boldsymbol{v}^T \left(\boldsymbol{B}_N^i - \left(\boldsymbol{Q}_N^i\right)^T\right)\boldsymbol{u}.
$$

where $\boldsymbol{v}, \boldsymbol{u}$ denotes the values of v and u at both volume and surface quadrature points.

Proof For convenience, let $\boldsymbol{u}_q, \boldsymbol{u}_f$ and $\boldsymbol{v}_q, \boldsymbol{v}_f$ denote evaluations of u and v at volume and surface points, such that

$$
\boldsymbol{u} = \begin{pmatrix}\boldsymbol{u}_q \\ \boldsymbol{u}_f\end{pmatrix}, \qquad \boldsymbol{v} = \begin{pmatrix}\boldsymbol{v}_q \\ \boldsymbol{v}_f\end{pmatrix}.
$$

The proof of the variational summation by parts property uses the definition of $\boldsymbol{Q}_N^i$ (7),

$$
\boldsymbol{v}^T \boldsymbol{Q}_N^i \boldsymbol{u} = \boldsymbol{v}_q^T \boldsymbol{Q}_i \boldsymbol{u}_q - \frac{1}{2}\left(\boldsymbol{E}\boldsymbol{v}_q\right)^T \boldsymbol{B}^i \left(\boldsymbol{E}\boldsymbol{u}_q\right) + \frac{1}{2}\left(\boldsymbol{E}\boldsymbol{v}_q\right)^T \boldsymbol{B}^i \boldsymbol{u}_f
$$

$$
- \frac{1}{2}\boldsymbol{v}_f^T \boldsymbol{B}^i \left(\boldsymbol{E}\boldsymbol{u}_q\right) + \frac{1}{2}\boldsymbol{v}_f^T \boldsymbol{B}^i \boldsymbol{u}_f.
$$

Applying Lemma 1 then yields

$$
\boldsymbol{v}^T \boldsymbol{Q}_N^i \boldsymbol{u} = -\boldsymbol{v}_q^T \boldsymbol{Q}_i^T \boldsymbol{u}_q + \frac{1}{2}\left(\boldsymbol{E}\boldsymbol{v}_q\right)^T \boldsymbol{B}^i \left(\boldsymbol{E}\boldsymbol{u}_q\right) + \frac{1}{2}\left(\boldsymbol{E}\boldsymbol{v}_q\right)^T \boldsymbol{B}^i \boldsymbol{u}_f
$$

$$
- \frac{1}{2}\boldsymbol{v}_f^T \boldsymbol{B}^i \left(\boldsymbol{E}\boldsymbol{u}_q\right) - \frac{1}{2}\boldsymbol{v}_f^T \boldsymbol{B}^i \boldsymbol{u}_f + \boldsymbol{v}_f^T \boldsymbol{B}^i \boldsymbol{u}_f
$$

$$
= \begin{pmatrix}\boldsymbol{v}_q \\ \boldsymbol{v}_f\end{pmatrix}^T \left(\begin{pmatrix}\boldsymbol{0} & \\ & \boldsymbol{B}^i\end{pmatrix} + \begin{pmatrix}-\boldsymbol{Q}_i^T + \frac{1}{2}\boldsymbol{E}^T \boldsymbol{B}^i \boldsymbol{E} & -\frac{1}{2}\left(\boldsymbol{B}^i \boldsymbol{E}\right)^T \\ \frac{1}{2}\boldsymbol{B}^i \boldsymbol{E} & -\frac{1}{2}\boldsymbol{B}^i\end{pmatrix}\right)\begin{pmatrix}\boldsymbol{u}_q \\ \boldsymbol{u}_f\end{pmatrix}
$$

$$
= \boldsymbol{v}^T \left(\boldsymbol{B}_N^i - \left(\boldsymbol{Q}_N^i\right)^T\right)\boldsymbol{u}.
$$

5.3 Entropy stability on a reference element

In this section, we construct so-called "entropy stable" schemes on the reference element $\widehat{D}$. These methods ensure that the entropy inequality (3) is satisfied discretely by avoiding the use of the chain rule in the proof of entropy dissipation. Entropy stable schemes rely on two main ingredients: an entropy stable numerical flux as defined by Tadmor [27] and a concept referred to as "flux differencing". Let $\boldsymbol{f}_S\left(\boldsymbol{u}_L, \boldsymbol{u}_R\right)$ be a numerical flux function which is a function of "left" and "right" states $\boldsymbol{u}_L, \boldsymbol{u}_R$. The numerical flux $\boldsymbol{f}_S$ is *entropy conservative* if it satisfies the following three conditions:

$$\boldsymbol{f}_S^i(\boldsymbol{u}, \boldsymbol{u}) = \boldsymbol{f}_i(\boldsymbol{u}), \qquad \text{(consistency)} \tag{10}$$

$$\boldsymbol{f}_S^i(\boldsymbol{u}_L, \boldsymbol{u}_R) = \boldsymbol{f}_S^i(\boldsymbol{u}_R, \boldsymbol{u}_R), \qquad \text{(symmetry)}$$

$$(\boldsymbol{v}_L - \boldsymbol{v}_R)^T \boldsymbol{f}_S^i(\boldsymbol{u}_L, \boldsymbol{u}_R) = \psi_i(\boldsymbol{u}_L) - \psi_i(\boldsymbol{u}_R), \qquad \text{(conservation)}$$

for $j = 1, \ldots, d$. The construction of entropy stable schemes will utilize (5.3) in discretizations of both volume and surface terms in a DG formulation.

Proving a semi-discrete entropy inequality typically involves the "strong" SBP condition. The schemes presented in this work will relax this, and use only two (weaker) conditions: that the decoupled SBP operator $\boldsymbol{D}_N^i$ exactly differentiates constants and that a discrete form of the fundamental theorem of calculus (FTC) holds. The latter property can be derived from the variational SBP property in Lemma 2.

Lemma 3 *(Discrete FTC and exact differentiation of constants) Suppose Assumption 1 holds for $v(\boldsymbol{x}) = 1$. Let $u(\boldsymbol{x})$ be some L^2 integrable function, and let $\boldsymbol{u}$ denote the vector of values of $u(\boldsymbol{x})$ at volume and surface quadrature points. Then,*

$$\boldsymbol{1}^T \boldsymbol{Q}_N^i \boldsymbol{u} = \boldsymbol{1}^T \boldsymbol{B}_N^i \boldsymbol{u}, \qquad \boldsymbol{Q}_N^i \boldsymbol{1} = \boldsymbol{0}.$$

Proof The proof that $\boldsymbol{Q}_N^i \boldsymbol{1} = \boldsymbol{0}$ follows from the property that polynomials are equal to their L^2 projection, and is identical to that of [6,7]. The proof of the first equality follows from $\boldsymbol{Q}_N^i \boldsymbol{1} = \boldsymbol{0}$ and Lemma 2

$$\boldsymbol{1}^T \left(\boldsymbol{Q}_N^i\right) \boldsymbol{u} = \boldsymbol{1}^T \left(\boldsymbol{B}_N^i - \left(\boldsymbol{Q}_N^i\right)^T\right) \boldsymbol{u} = \boldsymbol{1}^T \boldsymbol{B}_N^i \boldsymbol{u}.$$

We can now construct a skew-symmetric formulation on the reference element $\widehat{D}$ and show that it is semi-discretely entropy conservative. This formulation can be made entropy stable by adding interface dissipation. Let $\boldsymbol{u}_h$ denote the discrete solution, and let $\boldsymbol{u}_q$ denote the values of the solution at volume quadrature points. We define the auxiliary conservative variables $\widetilde{\boldsymbol{u}}$ in terms of the L^2 projections of the entropy variables

$$\boldsymbol{v}_q = \boldsymbol{v}\left(\boldsymbol{u}_q\right), \qquad \widetilde{\boldsymbol{v}} = \begin{bmatrix} \boldsymbol{V}_q \\ \boldsymbol{V}_f \end{bmatrix} \boldsymbol{P}_q \boldsymbol{v}_q, \qquad \widetilde{\boldsymbol{u}} = \boldsymbol{u}\left(\widetilde{\boldsymbol{v}}\right). \tag{11}$$

The skew-symmetric formulation for (1) on $\widehat{D}$ is given in terms of $\widetilde{\boldsymbol{u}}$

$$\boldsymbol{M} \frac{\partial \boldsymbol{u}_h}{\partial t} + \sum_{i=1}^d \begin{bmatrix} \boldsymbol{V}_q \\ \boldsymbol{V}_f \end{bmatrix}^T \left(\left(\boldsymbol{Q}_N^i - \left(\boldsymbol{Q}_N^i\right)^T\right) \circ \boldsymbol{F}_S^i\right) \boldsymbol{1} + \boldsymbol{V}_f^T \boldsymbol{B}^i \boldsymbol{f}_i^* = 0, \tag{12}$$

$$\left(\boldsymbol{F}_S^i\right)_{ij} = \boldsymbol{f}_S^i\left(\widetilde{\boldsymbol{u}}_i, \widetilde{\boldsymbol{u}}_j\right), \qquad 1 \leq i, j \leq N_q + N_q^f,$$

where $\boldsymbol{f}^*$ is some numerical flux, and the matrix $\left(\boldsymbol{Q}_N^i - \left(\boldsymbol{Q}_N^i\right)^T\right)$ possesses the following block structure:

$$\left(\boldsymbol{Q}_N^i - \left(\boldsymbol{Q}_N^i\right)^T\right) = \begin{pmatrix} \boldsymbol{Q}_i - \boldsymbol{Q}_i^T & \boldsymbol{E}^T\boldsymbol{B}^i \\ -\boldsymbol{B}^i\boldsymbol{E} & \boldsymbol{0} \end{pmatrix}.$$

Multiplying the formulation (12) by $\boldsymbol{M}^{-1}$ on both sides yields a strong form

$$\frac{\partial \boldsymbol{u}_h}{\partial t} + \sum_{i=1}^d \left[\, \boldsymbol{P}_q \ \boldsymbol{L}_f \,\right] \left(\left(\boldsymbol{D}_N^i - \boldsymbol{W}_N^{-1}\left(\boldsymbol{Q}_N^i\right)^T\right) \circ \boldsymbol{F}_S^i\right) \boldsymbol{1} + \boldsymbol{L}_f \mathrm{diag}\left(\widehat{\boldsymbol{n}}_i\right) \boldsymbol{f}_i^* = 0, \ (13)$$

We can now show that the skew-symmetric formulation is entropy conservative.

Theorem 2 *Suppose Assumption 1 holds for $v(\boldsymbol{x}) = 1$. Then, the formulation (12) is entropy conservative such that*

$$\boldsymbol{1}^T\boldsymbol{W}\frac{\partial U(\boldsymbol{u}_q)}{\partial t} + \sum_{i=1}^d \boldsymbol{1}^T\boldsymbol{B}^i\left(\widetilde{\boldsymbol{v}}_f^T\boldsymbol{f}_i^* - \psi_i(\widetilde{\boldsymbol{u}}_f)\right) = 0, \qquad \boldsymbol{u}_q = \boldsymbol{V}_q\boldsymbol{u}. \qquad (14)$$

Proof Testing (12) by $\boldsymbol{v}_h = \boldsymbol{P}_q\boldsymbol{v}_q$ yields

$$\boldsymbol{v}_q^T\boldsymbol{W}\frac{\partial \left(\boldsymbol{V}_q\boldsymbol{u}\right)}{\partial t} + \sum_{i=1}^d \widetilde{\boldsymbol{v}}^T\left(\left(\boldsymbol{Q}_N^i - \left(\boldsymbol{Q}_N^i\right)^T\right) \circ \boldsymbol{F}_S^i\right) \boldsymbol{1} + \widetilde{\boldsymbol{v}}_f^T\boldsymbol{B}^i\boldsymbol{f}_i^* = 0. \qquad (15)$$

Algebraic manipulations (see [6] for details) yields that

$$\widetilde{\boldsymbol{v}}^T\left(\left(\boldsymbol{Q}_N^i - \left(\boldsymbol{Q}_N^i\right)^T\right) \circ \boldsymbol{F}_S^i\right) \boldsymbol{1} = \widetilde{\boldsymbol{v}}^T\left(\boldsymbol{Q}_N^i \circ \boldsymbol{F}_S^i\right) \boldsymbol{1} - \widetilde{\boldsymbol{v}}^T\left(\left(\boldsymbol{Q}_N^i\right)^T \circ \boldsymbol{F}_S^i\right) \boldsymbol{1}$$

$$= \widetilde{\boldsymbol{v}}^T\left(\boldsymbol{Q}_N^i \circ \boldsymbol{F}_S^i\right) \boldsymbol{1} - \boldsymbol{1}^T\left(\boldsymbol{Q}_N^i \circ \boldsymbol{F}_S^i\right) \widetilde{\boldsymbol{v}}.$$

Where we have used that $\boldsymbol{F}_S^i$ is symmetric and that the Hadamard product commutes. Applying the conservation condition on $\boldsymbol{f}_S^i$ in (5.3) then yields

$$\widetilde{\boldsymbol{v}}^T\left(\boldsymbol{Q}_N^i \circ \boldsymbol{F}_S^i\right) \boldsymbol{1} - \boldsymbol{1}^T\left(\boldsymbol{Q}_N^i \circ \boldsymbol{F}_S^i\right) \widetilde{\boldsymbol{v}}$$

$$= \sum_{jk}\left(\boldsymbol{Q}_N^i\right)_{jk}\left(\widetilde{\boldsymbol{v}}_j - \widetilde{\boldsymbol{v}}_k\right)\boldsymbol{f}_S\left(\widetilde{\boldsymbol{u}}_j, \widetilde{\boldsymbol{u}}_k\right) = \sum_{jk}\left(\boldsymbol{Q}_N^i\right)_{jk}\left(\psi_i(\widetilde{\boldsymbol{u}}_j) - \psi_i(\widetilde{\boldsymbol{u}}_k)\right)$$

$$= \boldsymbol{1}^T\left(\boldsymbol{Q}_N^i\right)\psi_i(\widetilde{\boldsymbol{u}}) - \psi_i(\widetilde{\boldsymbol{u}})^T\left(\boldsymbol{Q}_N^i\right)\boldsymbol{1} = \boldsymbol{1}^T\left(\boldsymbol{Q}_N^i\right)\psi_i(\widetilde{\boldsymbol{u}}) = \boldsymbol{1}^T\boldsymbol{B}_N^i\psi_i(\widetilde{\boldsymbol{u}}),$$

where we have used Lemma 3 in the last equality. Noting that $\boldsymbol{1}^T\boldsymbol{B}_N^i\psi_i(\widetilde{\boldsymbol{u}}) = \boldsymbol{1}^T\boldsymbol{B}^i\psi_i(\widetilde{\boldsymbol{u}}_f)$ completes the proof.

Remark 2 The primary difference between this formulation and the formulation presented in [6] is the use of the skew-symmetric volume operator $\left(\boldsymbol{Q}_N^i - \left(\boldsymbol{Q}_N^i\right)^T\right)$. When the strong SBP property (9) holds, this formulation is exactly equivalent to the strong formulation presented in [6]. However, the only result necessary to prove Theorem 2 is Lemma 3. The decoupled SBP property (9) is not utilized, and is not necessary to guarantee a semi-discrete conservation of entropy for the skew-symmetric formulation.

The skew symmetric formulation can also be shown to be locally conservative in the sense of [28], which is sufficient to show the numerical solution convergences to the weak solution under mesh refinement.

Theorem 3 *The formulation (12) is locally conservative such that*

$$\mathbf{1}^T \boldsymbol{W} \frac{\partial \left(\boldsymbol{V}_q \boldsymbol{u}\right)}{\partial t} + \sum_{i=1}^{d} \mathbf{1}^T \boldsymbol{B}^i \boldsymbol{f}_i^* = 0. \tag{16}$$

Proof To show local conservation, we test (12) with 1

$$\mathbf{1}^T \boldsymbol{W} \boldsymbol{V}_q \frac{\partial \boldsymbol{u}_h}{\partial t} + \sum_{i=1}^{d} \mathbf{1}^T \left(\left(\boldsymbol{Q}_N^i - \left(\boldsymbol{Q}_N^i\right)^T\right) \circ \boldsymbol{F}_S\right) \mathbf{1} + \mathbf{1}^T \boldsymbol{W}_f \mathrm{diag}\left(\widehat{\boldsymbol{n}}\right) \boldsymbol{f}_i^* = 0. \tag{17}$$

Because $\boldsymbol{F}_S$ is symmetric and $\left(\boldsymbol{Q}_N^i - \left(\boldsymbol{Q}_N^i\right)^T\right)$ is skew-symmetric, their Hadamard product is also skew-symmetric. Using that $\boldsymbol{x}^T \boldsymbol{A} \boldsymbol{x} = 0$ for any skew symmetric matrix $\boldsymbol{A}$, the volume term $\mathbf{1}^T \left(\left(\boldsymbol{Q}_N^i - \left(\boldsymbol{Q}_N^i\right)^T\right) \circ \boldsymbol{F}_S\right) \mathbf{1}$ vanishes.

5.4 On quadrature conditions for Assumption 1 with $v = 1$

Apart from algebraic manipulations, only Lemma 3 is necessary to prove entropy conservation for (13). Lemma 3 requires that Assumption 1 holds for $v = 1$. Thus, the volume and surface quadratures must be sufficiently accurate to guarantee that the mass matrix is positive definite and to integrate

$$\int_{\widehat{D}} \frac{\partial u}{\partial x_i}, \qquad \int_{\partial \widehat{D}} u \widehat{n}_i. \tag{18}$$

On simplicial elements, the mass matrix is guaranteed to be positive definite for any volume quadrature which is exact for degree $2N$ polynomial integrands. This choice of volume quadrature also guarantees that the volume term in (18) is integrated exactly. The surface quadrature can thus be taken to be any quadrature rule which is exact for only degree N integrands on faces. In contrast, the construction of simplicial decoupled SBP operators has required face quadratures which are accurate for degree $2N$ polynomials [6, 7].

On tensor product elements, we can take any degree $(2N - 1)$ quadrature rule which ensures a positive definite mass matrix (e.g. a $(N + 1)$-point GLL quadrature), as a quadrature of this accuracy is sufficient to exactly integrate the volume term in (18). For the surface quadrature, we can again take any quadrature rule which is exact for degree N polynomial integrands. For example, on a quadrilateral element, one can use $\left\lceil \frac{N+1}{2} \right\rceil$-point Gauss quadrature rule or a $\left\lceil \frac{N+3}{2} \right\rceil$-point GLL rule as face quadratures for a degree N scheme.

6 Skew-symmetric entropy conservative formulations on mapped elements

We now construct skew-symmetric formulations on mapped elements. We assume some domain Ω is decomposed into non-overlapping elements D^k, such that D^k is the image of the reference element $\widehat{D}$ under an isoparametric mapping $\boldsymbol{\Phi}^k$. We define geometric change of variables terms G_{ij}^k as scaled derivatives of reference coordinates $\widehat{\boldsymbol{x}}$ w.r.t. physical coordinates $\boldsymbol{x}$

$$\frac{\partial u}{\partial x_i} = \sum_{ij} G_{ij}^k \frac{\partial u}{\partial \widehat{x}_j}, \qquad G_{ij}^k = J^k \frac{\partial \widehat{x}_j}{\partial x_i}, \tag{19}$$

where J^k is the determinant of the Jacobian of the geometric mapping on the element D^k. We also introduce the scaled outward normal components $n_i J_f^k$, which can be computed in terms of (19) and the reference normals $\widehat{\boldsymbol{n}}$ on $\widehat{D}$

$$n_i^k J_f^k = \sum_{j=1}^d G_{ij}^k \widehat{n}_j. \tag{20}$$

We also define $\boldsymbol{n}_i^k$ as the vector containing concatenated values of the scaled outward normals $n_i^k J_f^k$ at surface quadrature nodes. For the remainder of the work, we assume that the mesh is watertight [7] such that at all points on any internal face, the scaled outward normals $n_i^k J_f^k$ on the two elements sharing this face are equal and opposite.

On a single element (and on affine meshes), it is possible to show entropy stability of the skew-symmetric formulation (12) under a surface quadrature which is only exact for degree N polynomials. However, on curved meshes, stronger conditions are required to guarantee entropy stability. This is due to the fact that the geometric terms are now high order polynomials which vary spatially over each element. Moreover, Lemma 3 assumes affine geometric mappings, and does not hold on curved elements. In this section, we discuss how to extend Lemma 3 to curved simplicial and tensor product elements.

6.1 Curved elements and the geometric conservation law

In this section, we describe how to construct appropriate decoupled SBP operators on curved meshes, and give conditions on the volume and surface quadrature rules under which a semi-discretely entropy stable scheme can be constructed.

We first show how to construct decoupled SBP operators on curved elements. Let $\boldsymbol{G}_{ij}^k$ denote the vector of scaled geometric terms G_{ij}^k evaluated at both volume and surface quadrature points, and let $\widehat{\boldsymbol{D}}_N^j$ denote the decoupled SBP operator for the jth reference coordinate. Decoupled SBP operators on a curved element D^k can be defined as in [7] by

$$\boldsymbol{D}_k^i = \frac{1}{2} \sum_{j=1}^d \left(\mathrm{diag}\left(\boldsymbol{G}_{ij}^k \right) \widehat{\boldsymbol{D}}_N^j + \widehat{\boldsymbol{D}}_N^j \mathrm{diag}\left(\boldsymbol{G}_{ij}^k \right) \right), \qquad \boldsymbol{Q}_k^i = \boldsymbol{W} \boldsymbol{D}_k^i. \tag{21}$$

It can be shown that, if $\widehat{\boldsymbol{D}}_N^j$ satisfies a strong summation by parts property, $\boldsymbol{D}_k^i$ satisfies an analogous strong summation by parts property.

For curved elements, steps must also be taken to ensure that the analogue of Lemma 2 and Lemma 3 hold at the discrete level. Expanding out the condition $\boldsymbol{Q}_k^i \mathbf{1} = \mathbf{0}$ in terms of (21) yields

$$\boldsymbol{Q}_k^i \mathbf{1} = \frac{1}{2} \boldsymbol{W} \sum_{j=1}^d \mathrm{diag}\left(\boldsymbol{G}_{ij}^k\right) \widehat{\boldsymbol{D}}_N^j \mathbf{1} + \widehat{\boldsymbol{D}}_N^j \mathrm{diag}\left(\boldsymbol{G}_{ij}^k\right) \mathbf{1} = \frac{1}{2} \boldsymbol{W} \sum_{j=1}^d \widehat{\boldsymbol{D}}_N^j \left(\boldsymbol{G}_{ij}^k\right) = 0,$$
(22)

where we have used that $\widehat{\boldsymbol{D}}_N^j \mathbf{1} = 0$. We refer to the condition $\boldsymbol{Q}_k^i \mathbf{1} = 0$ as the discrete geometric conservation law (GCL) [29, 30]. For degree N isoparametric mappings, the GCL is automatically satisfied in two dimensions due to the fact that the exact geometric terms G_{ij}^k are polynomials of degree N [30]. However, in three dimensions, the GCL is not automatically satisfied due to the fact that the degree of G_{ij}^k is larger than N. Thus, the geometric terms cannot be represented exactly using degree N polynomials, and (22) must be enforced through an alternative construction of G_{ij}^k.

To ensure that the geometric terms satisfy the GCL, we first rewrite the geometric terms as the curl of some quantity $\boldsymbol{r}^i$, but interpolate $\boldsymbol{r}^i$ before applying the curl [7, 30–32]:

$$\boldsymbol{r}^i = \frac{\partial \boldsymbol{x}}{\partial \widehat{x}_i} \times \boldsymbol{x}, \qquad \begin{bmatrix} G_{1j}^k \\ G_{2j}^k \\ G_{3j}^k \end{bmatrix} = \begin{bmatrix} \left(-\widehat{\nabla} \times I_{N_{\mathrm{geo}}}\left(x_3 \widehat{\nabla} x_2\right)\right)_j \\ \left(\widehat{\nabla} \times I_{N_{\mathrm{geo}}}\left(x_3 \widehat{\nabla} x_1\right)\right)_j \\ \left(\widehat{\nabla} \times I_{N_{\mathrm{geo}}}\left(x_1 \widehat{\nabla} x_2\right)\right)_j \end{bmatrix}, \qquad (23)$$

$$N_{\mathrm{geo}} \leq \begin{cases} N+1 & \text{(tetrahedra)} \\ N & \text{(hexahedra)} \end{cases},$$

where $I_{N_{\mathrm{geo}}}$ denotes a degree N_{geo} polynomial interpolation operator with appropriate interpolation nodes.[1] The restriction on the maximum value of N_{geo} ensures that $G_{ij}^k \in V^N$ (e.g. $G_{ij}^k \in P^N$ on tetrahedral elements and $G_{ij}^k \in Q^N$ on hexahedral elements), which is also necessary to guarantee (22).

Because the decoupled SBP operators $\boldsymbol{D}_k^i$ are now defined through (21), Lemma 3 and the proof of entropy stability no longer hold for curved elements and must be modified. The introduction of curvilinear meshes will impose slightly different conditions on the accuracy of the surface quadrature. We discuss simplicial and tensor product elements separately, as differences in the natural polynomial approximation spaces will result in different assumptions for each proof.

Lemma 4 (*Discrete FTC and exact constant differentiation on curved elements*) *Let D^k be a curved element, and let the geometric terms G_{ij}^k be constructed using (6.1). Let Assumption 1 hold for $v = 1$ and $v = G_{ij}^k$ for all $i, j = 1, \ldots, d$, and let $\boldsymbol{u}$ denote a vector of values of some function at volume and surface quadrature points. Then,*

$$\mathbf{1}^T \boldsymbol{Q}_k^i \boldsymbol{u} = \mathbf{1}^T B_k^i \boldsymbol{u}, \qquad \boldsymbol{Q}_k^i \mathbf{1} = \mathbf{0},$$

---

[1] This interpolation step must be performed using interpolation points with an appropriate number of nodes on each boundary [7]. These include, for example, GLL nodes on tensor product elements, and optimized interpolation nodes on non-tensor product elements [33–35].

where the physical boundary matrix $\boldsymbol{B}_k^i$ is defined as

$$\boldsymbol{B}_k^i = \sum_{j=1}^d \boldsymbol{B}_N^j \operatorname{diag}\left(\boldsymbol{G}_{ij}^k\right) = \sum_{j=1}^d \operatorname{diag}\left(\boldsymbol{G}_{ij}^k\right) \boldsymbol{B}_N^j = \begin{pmatrix} \boldsymbol{0} \\ \boldsymbol{W}_f \operatorname{diag}\left(\boldsymbol{n}_i^k\right) \end{pmatrix}.$$

Proof The proof of $\boldsymbol{Q}_k^i \boldsymbol{1} = \boldsymbol{0}$ was shown for for tensor product elements in [30] and for simplicial elements in [7], and relies only on the fact that $G_{ij}^k \in V^N$.

The discrete fundamental theorem of calculus $\boldsymbol{1}^T \boldsymbol{Q}_k^i \boldsymbol{u} = \boldsymbol{1}^T \boldsymbol{B}_k^i \boldsymbol{u}$ can be shown to hold using (21):

$$\boldsymbol{1}^T \boldsymbol{Q}_k^i \boldsymbol{u} = \frac{1}{2} \sum_{j=1}^d \boldsymbol{1}^T \left(\operatorname{diag}\left(\boldsymbol{G}_{ij}^k\right) \widehat{\boldsymbol{Q}}_N^j + \widehat{\boldsymbol{Q}}_N^j \operatorname{diag}\left(\boldsymbol{G}_{ij}^k\right) \right) \boldsymbol{u}$$

$$= \frac{1}{2} \sum_{j=1}^d \left(\left(\boldsymbol{G}_{ij}^k\right)^T \widehat{\boldsymbol{Q}}_N^j \boldsymbol{u} + \boldsymbol{1}^T \widehat{\boldsymbol{Q}}_N^j \operatorname{diag}\left(\boldsymbol{G}_{ij}^k\right) \boldsymbol{u} \right).$$

Applying Lemma 2 to $\sum_{j=1}^d \boldsymbol{1}^T \widehat{\boldsymbol{Q}}_N^j \operatorname{diag}\left(\boldsymbol{G}_{ij}^k\right) \boldsymbol{u}$ yields

$$\sum_{j=1}^d \boldsymbol{1}^T \widehat{\boldsymbol{Q}}_N^j \operatorname{diag}\left(\boldsymbol{G}_{ij}^k\right) \boldsymbol{u} = \sum_{j=1}^d \boldsymbol{1}^T \left(\boldsymbol{B}_N^j - \left(\widehat{\boldsymbol{Q}}_N^j\right)^T \right) \operatorname{diag}\left(\boldsymbol{G}_{ij}^k\right) \boldsymbol{u}$$

$$= \sum_{j=1}^d \boldsymbol{1}^T \boldsymbol{B}_N^j \operatorname{diag}\left(\boldsymbol{G}_{ij}^k\right) \boldsymbol{u},$$

where we have used Lemma 3 to conclude that $\widehat{\boldsymbol{Q}}_N^j \boldsymbol{1} = 0$. Repeating the procedure for $\sum_{j=1}^d \left(\boldsymbol{G}_{ij}^k\right)^T \widehat{\boldsymbol{Q}}_N^j \boldsymbol{u}$ yields

$$\sum_{j=1}^d \left(\boldsymbol{G}_{ij}^k\right)^T \widehat{\boldsymbol{Q}}_N^j \boldsymbol{u} = \sum_{j=1}^d \left(\boldsymbol{G}_{ij}^k\right)^T \left(\boldsymbol{B}_N^j - \left(\widehat{\boldsymbol{Q}}_N^j\right)^T \right) \boldsymbol{u}$$

$$= \sum_{j=1}^d \left(\boldsymbol{G}_{ij}^k\right)^T \boldsymbol{B}_N^j \boldsymbol{u} - \sum_{j=1}^d \boldsymbol{u}^T \widehat{\boldsymbol{Q}}_N^j \boldsymbol{G}_{ij}^k = \sum_{j=1}^d \left(\boldsymbol{G}_{ij}^k\right)^T \boldsymbol{B}_N^j \boldsymbol{u},$$

where we have used that the G_{ij}^k satisfies the discrete GCL. The proof is completed by noting that $\boldsymbol{B}_N^j$ is diagonal and thus commutes with $\operatorname{diag}\left(\boldsymbol{G}_{ij}^k\right)$, such that

$$\boldsymbol{1}^T \boldsymbol{Q}_k^i \boldsymbol{u} = \sum_{j=1}^d \boldsymbol{1}^T \left(\boldsymbol{B}_N^j \operatorname{diag}\left(\boldsymbol{G}_{ij}^k\right) \right) \boldsymbol{u} = \boldsymbol{1}^T \boldsymbol{B}_k^i \boldsymbol{u}.$$

The property $\boldsymbol{Q}_k^i \boldsymbol{1} = 0$ is also related to free-stream preservation [30]. Constant solutions are stationary solutions of systems of conservation laws. However, on curved meshes, the presence of spatially varying geometric terms can result in the production of spurious transient waves. The construction of geometric terms through (6.1) guarantees that the resulting methods are free-stream preserving, and that constant solutions remain stationary solutions of discretizations of (1).

We can now construct and prove entropy conservation and free stream preservation for a skew-symmetric formulation on a curved element D^k. Let $\boldsymbol{Q}_k^i$ be given by (21), and define the curved mass matrix $\boldsymbol{M}^k = \boldsymbol{V}_q^T \boldsymbol{W} \operatorname{diag}\left(\boldsymbol{J}^k\right) \boldsymbol{V}_q$. Note that $\boldsymbol{M}^k$ is positive-definite so long as J^k is positive at all quadrature points. We define the auxiliary quantities $\widetilde{\boldsymbol{u}}$

$$
\boldsymbol{v}_q = \boldsymbol{v}\left(\boldsymbol{u}_q\right), \qquad \widetilde{\boldsymbol{v}} = \begin{bmatrix} \boldsymbol{V}_q \\ \boldsymbol{V}_f \end{bmatrix} \boldsymbol{P}_q^k \boldsymbol{v}_q, \qquad \widetilde{\boldsymbol{u}} = \boldsymbol{u}\left(\widetilde{\boldsymbol{v}}\right).
$$

where $\boldsymbol{P}_q^k = \left(\boldsymbol{M}^k\right)^{-1} \boldsymbol{V}_q^T \boldsymbol{W} \operatorname{diag}\left(\boldsymbol{J}^k\right)$. Then, we have the following theorem:

Theorem 4 *Let the geometric terms G_{ij}^k be computed from (6.1), let the scaled outward normals $\boldsymbol{n}_i^k$ be computed pointwise from (20), and suppose Assumption 1 holds for $v = 1$ and $v = G_{ij}^k$. Let $\widetilde{\boldsymbol{u}}_f^+$ denote the face value of the entropy-projected conservative variables $\widetilde{\boldsymbol{u}}_f$ on the neighboring element. Then, the formulation*

$$
\boldsymbol{M}^k \frac{\partial \boldsymbol{u}_h}{\partial t} + \sum_{i=1}^d \begin{bmatrix} \boldsymbol{V}_q \\ \boldsymbol{V}_f \end{bmatrix}^T \left(\left(\boldsymbol{Q}_k^i - \left(\boldsymbol{Q}_k^i\right)^T\right) \circ \boldsymbol{F}_S^i\right) \mathbf{1} + \boldsymbol{V}_f^T \boldsymbol{W}_f \operatorname{diag}\left(\boldsymbol{n}_i^k\right) \boldsymbol{f}_i^* = 0,
$$

$$
\text{(24)}
$$

$$
\left(\boldsymbol{F}_S^i\right)_{ij} = \boldsymbol{f}_S^i\left(\widetilde{\boldsymbol{u}}_i, \widetilde{\boldsymbol{u}}_j\right), \qquad 1 \le i,j \le N_q + N_q^f,
$$

$$
\boldsymbol{f}_i^* = \boldsymbol{f}_S^i(\widetilde{\boldsymbol{u}}_f^+, \widetilde{\boldsymbol{u}}_f), \qquad \text{on interior interfaces,}
$$

is semi-discretely entropy conservative on D^k such that for $\boldsymbol{u}_q = \boldsymbol{V}_q \boldsymbol{u}$,

$$
\mathbf{1}^T \boldsymbol{W} \operatorname{diag}\left(\boldsymbol{J}^k\right) \frac{\partial U(\boldsymbol{u}_q)}{\partial t} + \sum_{i=1}^d \mathbf{1}^T \boldsymbol{W}_f \operatorname{diag}\left(\boldsymbol{n}_i^k\right) \left(\psi_i(\widetilde{\boldsymbol{u}}_f) - \widetilde{\boldsymbol{v}}_f^T \boldsymbol{f}_i^*\right) = 0.
$$

Additionally, the method is free-stream preserving such that $\frac{\partial \boldsymbol{u}_h}{\partial t} = 0$ for constant solutions.

Proof The proof of entropy stability is identical to that of Theorem 2, except that Lemma 4 is used instead of Lemma 3. However, proving free-stream preservation differs from approaches in the literature, which typically show that the right hand side is zero for $\boldsymbol{u}_h$ constant [4, 7]. This strategy for is appropriate for "strong" formulations, but must be modified for the skew-symmetric formulation (24).

We have that $\boldsymbol{f}_i^* = \boldsymbol{f}_S^i(\widetilde{\boldsymbol{u}}_f^+, \widetilde{\boldsymbol{u}}_f) = \boldsymbol{f}_i(\boldsymbol{u}_f)$ using the consistency property of the Tadmor flux (5.3) and the fact that the solution is globally constant. For $\boldsymbol{u}_h$ constant, $\boldsymbol{F}_S$ is also constant. We assume (without loss of generality) that $\boldsymbol{F}_S$ and $\boldsymbol{f}_i(\boldsymbol{u}_f)$ are the matrix and vector of ones, respectively. Then,

$$
\left(\left(\boldsymbol{Q}_k^i - \left(\boldsymbol{Q}_k^i\right)^T\right) \circ \boldsymbol{F}_S\right) \mathbf{1} = \left(\boldsymbol{Q}_k^i - \left(\boldsymbol{Q}_k^i\right)^T\right) \mathbf{1} = \left(\boldsymbol{Q}_k^i\right)^T \mathbf{1},
$$

where we have used that $\boldsymbol{Q}_k^i \boldsymbol{1} = 0$ by Lemma 4. Thus, the right hand side reduces to

$$
\sum_{j=1}^d \begin{bmatrix} \boldsymbol{V}_q \\ \boldsymbol{V}_f \end{bmatrix}^T \left(-\left(\boldsymbol{Q}_k^i\right)^T + \boldsymbol{V}_f^T \boldsymbol{W}_f \operatorname{diag}\left(\boldsymbol{n}_i^k\right) \right) \boldsymbol{1}
$$

$$
= \sum_{j=1}^d \begin{bmatrix} \boldsymbol{V}_q \\ \boldsymbol{V}_f \end{bmatrix}^T \left(\left(-\frac{1}{2}\left(\operatorname{diag}\left(\boldsymbol{G}_{ij}^k\right)\widehat{\boldsymbol{Q}}_N^j + \widehat{\boldsymbol{Q}}_N^j \operatorname{diag}\left(\boldsymbol{G}_{ij}^k\right) \right)^T + \widehat{\boldsymbol{B}}_N^j \operatorname{diag}\left(\boldsymbol{G}_{ij}^k\right) \right) \right) \boldsymbol{1},
$$

where we have used the definition of $\boldsymbol{Q}_k^i$ in (21). Rearranging terms gives that, for a constant solution, (24) reduces to

$$
\boldsymbol{M}^k \frac{\partial \boldsymbol{u}_h}{\partial t} + \frac{1}{2}\sum_{j=1}^d \begin{bmatrix} \boldsymbol{V}_q \\ \boldsymbol{V}_f \end{bmatrix}^T \left(-\left(\widehat{\boldsymbol{Q}}_N^j\right)^T + \widehat{\boldsymbol{B}}_N^j \right) \boldsymbol{G}_{ij}^k
$$

$$
+ \frac{1}{2}\sum_{j=1}^d \begin{bmatrix} \boldsymbol{V}_q \\ \boldsymbol{V}_f \end{bmatrix}^T \operatorname{diag}\left(\boldsymbol{G}_{ij}^k\right)\left(-\left(\widehat{\boldsymbol{Q}}_N^j\right)^T + \widehat{\boldsymbol{B}}_N^j \right) \boldsymbol{1} = 0.
$$

Let u denote the constant value of the solution such that the values of the solution at quadrature points is $u\boldsymbol{1}$. Multiplying both sides by the constant solution $\boldsymbol{u}_h^T$ yields that $\frac{1}{2}\frac{\partial}{\partial t}\left(\boldsymbol{u}_h^T \boldsymbol{M}^k \boldsymbol{u}_h\right)$ is equal to

$$
-\frac{u}{2}\sum_{j=1}^d \left(\boldsymbol{1}^T \left(-\left(\widehat{\boldsymbol{Q}}_N^j\right)^T + \widehat{\boldsymbol{B}}_N^j \right) \boldsymbol{G}_{ij}^k + \left(\boldsymbol{G}_{ij}^k\right)^T \left(-\left(\widehat{\boldsymbol{Q}}_N^j\right)^T + \widehat{\boldsymbol{B}}_N^j \right) \boldsymbol{1} \right).
$$

By assumption, Lemma 2 holds for test functions $\boldsymbol{1}$ and $\boldsymbol{G}_{ij}^k$, and the formulation reduces to

$$
\frac{1}{2}\frac{\partial}{\partial t}\left(\boldsymbol{u}_h^T \boldsymbol{M}^k \boldsymbol{u}_h\right) + \frac{u}{2}\sum_{j=1}^d \left(\boldsymbol{1}^T \widehat{\boldsymbol{Q}}_N^j \boldsymbol{G}_{ij}^k + \left(\boldsymbol{G}_{ij}^k\right)^T \widehat{\boldsymbol{Q}}_N^j \boldsymbol{1} \right) = 0.
$$

By construction, $\widehat{\boldsymbol{Q}}_N^j \boldsymbol{1} = 0$, and $\sum_{j=1}^d \boldsymbol{1}^T \widehat{\boldsymbol{Q}}_N^j \boldsymbol{G}_{ij}^k = 0$ since G_{ij}^k satisfies the GCL. This implies that the latter term vanishes and $\frac{\partial}{\partial t}\left(\boldsymbol{u}_h^T \boldsymbol{M}^k \boldsymbol{u}_h\right) = 0$ on D^k. Since $\boldsymbol{M}^k$ is symmetric and positive-definite, $\boldsymbol{u}_h^T \boldsymbol{M}^k \boldsymbol{u}_h$ is a norm on $\boldsymbol{u}_h$. Summing $\frac{\partial}{\partial t}\left(\boldsymbol{u}_h^T \boldsymbol{M}^k \boldsymbol{u}_h\right) = 0$ over all elements ensures that globally constant solutions are stationary and that $\frac{\partial \boldsymbol{u}_h}{\partial t} = 0$.

The proof of global entropy conservation follows from summing up (14) over all elements and noting that the surface terms cancel due to the symmetry and conservation properties of the Tadmor flux (5.3) [6]. The entropy conservative formulations presented in this work can be made entropy stable by adding appropriate interface dissipation, such as Lax-Friedrichs or matrix-based penalization terms [6, 14, 36].

Remark 3 The skew-symmetric operator $\boldsymbol{Q}_k^i - \left(\boldsymbol{Q}_k^i\right)^T$ in (24) can be rewritten as

$$\sum_{j=1}^d \text{diag}\left(\boldsymbol{G}_{ij}^k\right) \frac{1}{2}\left(\widehat{\boldsymbol{Q}}_N^j - \left(\widehat{\boldsymbol{Q}}_N^j\right)^T\right) + \frac{1}{2}\left(\widehat{\boldsymbol{Q}}_N^j - \left(\widehat{\boldsymbol{Q}}_N^j\right)^T\right) \text{diag}\left(\boldsymbol{G}_{ij}^k\right).$$

Thus, the volume terms in the skew-symmetric formulation may be applied using only the skew-symmetric part of the reference SBP operator $\widehat{\boldsymbol{Q}}_N^j$.

Remark 4 It is also possible to replace the curved mass matrix $\boldsymbol{M}^k$ with a more easily invertible weight-adjusted approximation while maintaining high order accuracy, entropy stability, and local conservation [7]. This approximation avoids the inversion of dense weighted L^2 mass matrices $\boldsymbol{M}^k$ on curved simplicial elements, but is generally unnecessary on tensor product elements as common choices of volume quadrature result in a diagonal (lumped) mass matrix [3, 5, 15].

7 Conditions on the accuracy of volume and surface quadrature rules

The previous sections outline minimal conditions under which entropy stability is guaranteed under a skew-symmetric formulation and a polynomial geometric mapping. In Section 7.1, we translate these minimial conditions into conditions on quadrature accuracy.

Additionally, while it is possible to maintain entropy stability under reduced accuracy quadratures, the accuracy of the resulting schemes depend on the accuracy of the volume and surface quadrature rules. We analyze the degree of accuracy expected based on the accuracy of different quadrature rules in Section 7.2.

7.1 On quadrature conditions for Assumption 1 for $v = 1$ and $v = G_{ij}^k$

Semi-discrete entropy conservation on curved meshes requires that Assumption 1 holds for $v = 1$ and $v = G_{ij}^k$. We discuss specific choices of volume and surface quadrature on for which this assumption is valid, and summarize the maximum degree N_{geo} of the polynomial geometric approximation under which entropy stability holds for common choices of volume and surface quadrature.

In order to ensure that the mass matrix is positive-definite in Assumption 1, the volume quadrature must be degree $2N$ in general on simplices. The following lemma summarizes expected behavior for surface quadrature rules of varying order:

Lemma 5 *Let $\widehat{D}$ be a simplex with volume quadrature which is exact for degree $2N$ polynomials. Let the surface quadrature be exact for polynomials of degree $M+N$. Then, the skew-symmetric formulation (24) is entropy stable for $N_{\text{geo}} \leq \min\left(N + 1, M + 1\right)$.*

Proof Entropy stability holds if Assumption 1 holds for $v = 1$ and $v = G_{ij}^k$. Simplicial elements require $N_{\text{geo}} \leq (N + 1)$ in order to guarantee that $G_{ij}^k \in P^{N_{\text{geo}}-1} \subset P^N$, which is necessary to satisfy the discrete GCL [7]. Then, for $u \in P^N$, $\frac{\partial u}{\partial \widehat{x}_j} \in P^{N-1}$, the integrands in Assumption 1 are $\frac{\partial u}{\partial \widehat{x}_j} v \in P^{N+N_{\text{geo}}-2}$

and $uvn_i \in P^{N+N_{\mathrm{geo}}-1}$ for $v = G_{ij}^k$. The volume quadrature exactly integrates the first integrand for $N_{\mathrm{geo}} \leq N + 1$, while the surface quadrature exactly integrates the second integrand for $M \geq N_{\mathrm{geo}} - 1$, or $N_{\mathrm{geo}} \leq M + 1$.

The situation is more complicated for curved tensor product elements. It was shown in Section 5.4 that tensor product quadratures of degree $(2N - 1)$ satisfy Assumption 1 holds for $v = 1$. However, in contrast to the simplicial case, it is not immediately clear that degree $(2N - 1)$ volume quadratures exactly integrate $\int_{\widehat{D}} \frac{\partial u}{\partial \widehat{x}_j} v$ for $v = G_{ij}^k$ for tensor product elements. The difference between simplicial and tensor product elements is the polynomial space in which the derivative lies. In contrast to the simplicial case, if $u \in Q^N$, $\frac{\partial u}{\partial \widehat{x}_j} \notin Q^{N-1}$. Consider the three-dimensional case with $u, v \in Q^N$ and $i = 1$. Then, differentiation reduces the polynomial degree in one coordinate but not others and $\frac{\partial u}{\partial \widehat{x}_1} \in Q^{N-1,N,N}$. As a result, $\frac{\partial u}{\partial \widehat{x}_j} v \notin Q^{2N-1}$, and a tensor product quadrature of degree $(2N-1)$ (in each coordinate) does not exactly integrate $\int_{\widehat{D}} \frac{\partial u}{\partial \widehat{x}_j} v$ for general $v \in Q^N$.

We address the quadrilateral case first:

Lemma 6 *Let $\widehat{D}$ be a quadrilateral. Suppose the volume quadrature be exact for degree $M + N$ polynomials, and that the surface quadrature be exact for polynomials of degree $M + N$. Then, the skew-symmetric formulation (24) is entropy stable for $N_{\mathrm{geo}} \leq \min(N, M + 1)$.*

Proof As in Lemma 5, entropy stability holds if Assumption 1 holds for $v = 1$ and $v = G_{ij}^k$. The case of $v = 1$ was addressed previously, and we focus on $v = G_{ij}^k$. We first characterize the polynomial degree of the geometric terms G_{ij}^k. In contrast to the simplicial case, tensor product elements require $N_{\mathrm{geo}} \leq N$ in order to ensure that $G_{ij}^k \in Q^{N,N}$ and that the discrete GCL is satisfied [30]. On a quadrilateral element with a degree N_{geo} geometric mapping, G_{ij}^k is

$$G_{11}^k = \frac{\partial x_2}{\partial \widehat{x}_2} \in Q^{N_{\mathrm{geo}}, N_{\mathrm{geo}}-1}, \qquad G_{12}^k = -\frac{\partial x_2}{\partial \widehat{x}_1} \in Q^{N_{\mathrm{geo}}-1, N_{\mathrm{geo}}},$$

$$G_{21}^k = -\frac{\partial x_1}{\partial \widehat{x}_2} \in Q^{N_{\mathrm{geo}}, N_{\mathrm{geo}}-1}, \qquad G_{22}^k = \frac{\partial x_1}{\partial \widehat{x}_1} \in Q^{N_{\mathrm{geo}}-1, N_{\mathrm{geo}}}.$$

Since $\frac{\partial u}{\partial \widehat{x}_1} \in Q^{N-1,N}$ and $\frac{\partial u}{\partial \widehat{x}_2} \in Q^{N,N-1}$

$$\frac{\partial u}{\partial \widehat{x}_i} G_{ij}^k \in Q^{N+N_{\mathrm{geo}}-1}.$$

The volume quadrature exactly integrates this integrand for $M \geq N_{\mathrm{geo}} - 1$.

We now consider the condition in Assumption 1 on the surface integrals $\int_{\partial \widehat{D}} uv\widehat{n}_j$ for $v = G_{ij}^k$. For left and right faces of the quadrilateral, $\widehat{n}_2 = 0$, so this condition reduces to ensuring that the quantity uG_{i1}^k is integrated exactly using quadrature for $i = 1, 2$. Since G_{i1}^k are degree $N_{\mathrm{geo}} - 1$ in the $\widehat{x}_2$ coordinate, G_{i1}^k is degree $N_{\mathrm{geo}} - 1$ and $uG_{i1}^k \widehat{n}_1 \in Q^{N+N_{\mathrm{geo}}-1}$ along the left and right faces. Similarly, $uG_{i2}^k \widehat{n}_2 \in Q^{N+N_{\mathrm{geo}}-1}$ along the top and bottom faces and are zero along the left and right faces. The surface quadrature rule exactly integrates such integrands for $M \geq N_{\mathrm{geo}} - 1$, or $N_{\mathrm{geo}} \leq M + 1$.

Existing proofs of entropy stability on quadrilaterals rely on $(N+1)$-point GLL volume and surface quadratures, which are exact for degree $2N-1$ polynomials. The novelty of Lemma 7 is that the proof holds for any combination of degree $2N-1$ volume and surface quadratures (for example, $(N+1)$-point GLL volume quadrature and an $(N-1)$-point Gauss surface quadrature).

We now consider the three-dimensional case. In contrast to the quadrilateral case, the GCL is not automatically satisfied for a degree $N_{\text{geo}} \leq N$ geometric mapping. Instead, GCL-satisfying geometric terms are approximated using (6.1). Expanding out the expression for G_{11}^k gives

$$G_{11}^k = \frac{\partial}{\partial \widehat{x}_3} I_{N_{\text{geo}}} \left(x_3 \frac{\partial x_2}{\partial \widehat{x}_2} \right) - \frac{\partial}{\partial \widehat{x}_2} I_{N_{\text{geo}}} \left(x_3 \frac{\partial x_2}{\partial \widehat{x}_3} \right) \in Q^{N_{\text{geo}}}.$$

Repeating for the other geometric terms, one can show that $G_{ij}^k \in Q^{N_{\text{geo}}}$ on hexahedral elements. Thus, if $u \in Q^N$, $\frac{\partial u}{\partial \widehat{x}_1} G_{i1}^k \in Q^{N+N_{\text{geo}}-1, N+N_{\text{geo}}, N+N_{\text{geo}}}$, and is only integrated exactly by volume quadratures of degree $(2N-1)$ for geometric degrees $N_{\text{geo}} \leq (N-1)$. Similarly, Assumption 1 does not hold under degree $(2N-1)$ surface quadratures unless $N_{\text{geo}} \leq (N-1)$, due to the fact that traces of G_{ij}^k are degree N_{geo} polynomials in each coordinate.[2] We summarize these findings in the following lemma for hexahedral elements:

Lemma 7 *Let $\widehat{D}$ be a hexahedral element, with geometric terms constructed using (6.1). Let the volume quadrature be exact for degree $M+N$ polynomials, and let the surface quadrature be exact for polynomials of degree $M+N$. Then, the skew-symmetric formulation (24) is entropy stable for $N_{\text{geo}} \leq \min(N, M)$.*

Most implementations on tensor product elements utilize volume and surface quadratures of either degree $(2N-1)$ or $2N$. We summarize below for different pairings of volume and surface quadrature the maximum degree N_{geo} under which Assumption 1 is satisfied and entropy stability is guaranteed:

1. On quadrilateral elements, Assumption 1 holds for $N_{\text{geo}} \leq N$ and any tensor product volume and surface quadratures of degree $(2N-1)$
2. On hexahedral elements, Assumption 1 holds for $N_{\text{geo}} \leq N-1$ and any tensor product volume and surface quadratures of degree $(2N-1)$. If the SBP property holds (e.g. for GLL quadrature, or for volume and surface quadratures of degree $2N$) then Assumption 1 holds for $N_{\text{geo}} \leq N$.

We note that the condition $N_{\text{geo}} \leq N-1$ is non-standard for tensor product elements. However, this condition is only necessary for entropy stability when $\boldsymbol{Q}^i$ does not satisfy a generalized SBP property (see Remark 1). To the author's knowledge, this setting has not been considered within the literature.

---

[2] It is possible to construct the geometric terms for $N_{\text{geo}} = N$ using a local H_{div} basis where

$$\boldsymbol{r}^i \in Q^{N-1,N,N} \times Q^{N,N-1,N} \times Q^{N,N,N-1}.$$

Then, the geometric terms satisfy $\nabla \times \boldsymbol{r}^i \in Q^{N,N-1,N-1} \times Q^{N-1,N,N-1} \times Q^{N-1,N-1,N}$ with traces in Q^{N-1}, and Assumption 1 holds under degree $(2N-1)$ volume and surface quadrature. This approach will be investigated in more detail in future work.

7.2 On the accuracy of the skew-symmetric formulation

It was shown in [5, 6] that the decoupled SBP operator can be interpreted as augmenting a volume approximation of the derivative with boundary correction terms. Let $f(\boldsymbol{x}), g(\boldsymbol{x})$ denote two L^2 integrable functions, and let $\boldsymbol{f}_N, \boldsymbol{g}_N$ denote the vectors of values of f, g at both volume and surface quadrature points. A degree N approximation $u \in V^N$ to $f\frac{\partial g}{\partial x_i}$ can be constructed via

$$\boldsymbol{M}\boldsymbol{u} = \begin{bmatrix} \boldsymbol{V}_q \\ \boldsymbol{V}_f \end{bmatrix}^T \operatorname{diag}\left(\boldsymbol{f}_N\right) \boldsymbol{Q}_N^i \boldsymbol{g}_N, \qquad \boldsymbol{f}_N = \begin{bmatrix} \boldsymbol{f}_q \\ \boldsymbol{f}_f \end{bmatrix}, \quad \boldsymbol{g}_N = \begin{bmatrix} \boldsymbol{g}_q \\ \boldsymbol{g}_f \end{bmatrix}, \qquad (25)$$

where $\boldsymbol{u}$ denotes the vector of coefficients for u.

This algebraic expression (28) can be reinterpreted as a quadrature approximation of a variational problem, which can be mapped to a physical element D^k. We seek to approximate $f\frac{\partial g}{\partial x_i}$ by $u \in V^N$ such that, $\forall v \in V^N$

$$\int_{D^k} uv = \int_{D^k} f\frac{\partial \Pi_N g}{\partial x_i} v + \int_{\partial D^k} (g - \Pi_N g)\left(\frac{fv + \Pi_N(fv)}{2}\right) n_i^k, \qquad (26)$$

where Π_N is the L^2 projection operator (6). Integrating half of the volume term by parts yields the skew-symmetric form of (26)

$$\int_{D^k} uv = \frac{1}{2}\int_{D^k} \left(f\frac{\partial \Pi_N g}{\partial x_i} v - g\frac{\partial \Pi_N(fv)}{\partial x_i} \right) \qquad (27)$$
$$+ \frac{1}{2}\int_{\partial D^k} \left(fgv + (g - \Pi_N g)(fv + \Pi_N(fv)) \right) n_i^k \qquad \forall v \in V^N,$$

which yields the matrix formulation

$$\boldsymbol{M}\boldsymbol{u} = \frac{1}{2} \begin{bmatrix} \boldsymbol{V}_q \\ \boldsymbol{V}_f \end{bmatrix}^T \operatorname{diag}\left(\boldsymbol{f}_N\right) \left(\boldsymbol{Q}_N^i - \left(\boldsymbol{Q}_N^i\right)^T + \boldsymbol{B}_N^i \right) \boldsymbol{g}_N \qquad (28)$$

The accuracy of the formulations (12) and (24) can be understood by analyzing the degree of polynomial exactness of (28) as an approximation of the derivative. Let $u(\boldsymbol{x})$ be a polynomial of degree $\leq N$ with coefficients $\boldsymbol{u}$, and let $\boldsymbol{u}_N = \begin{bmatrix} \boldsymbol{u}_q, \boldsymbol{u}_f \end{bmatrix}^T$ denote the values of $u(\boldsymbol{x})$ at volume and surface quadrature points. An approximation of $\frac{\partial u}{\partial x_i}$ can be computed by applying (28)

$$\frac{\partial u}{\partial x_i} \approx \frac{1}{2}\boldsymbol{M}^{-1} \begin{bmatrix} \boldsymbol{V}_q \\ \boldsymbol{V}_f \end{bmatrix}^T \left(\boldsymbol{Q}_N^i - \left(\boldsymbol{Q}_N^i\right)^T + \boldsymbol{B}_N^i \right) \boldsymbol{u}_N. \qquad (29)$$

From (29), it can be shown that when $\boldsymbol{Q}^i$ satisfies a generalized SBP property, the decoupled SBP operator (9) produces a degree N approximation to the derivative [6]. When $\boldsymbol{Q}^i$ does not satisfy a generalized SBP property, we have the following lemma on the accuracy of (29):

Lemma 8 *Suppose that the volume quadrature is exact for degree $M + N - 1$ polynomials on simplices, or for polynomials in $Q^{M+N-1,M+N,M+N}$ on tensor product elements. Furthermore, assume that the surface quadrature is exact for degree $M + N$ polynomials on simplices and $Q^{M+N,M+N}$ on tensor product elements. Then, the skew-symmetric approximation of the derivative (29) is exact for polynomials of degree M.*

Proof Suppose $u \in P^M$. Let $\boldsymbol{u}$ denote the polynomial coefficients of u, and let $\boldsymbol{e}$ denote the difference between $\boldsymbol{D}^i \boldsymbol{u}$ (the exact coefficients of $\frac{\partial u}{\partial x_i}$) and the approximation (29)

$$\boldsymbol{e} = \boldsymbol{D}^i \boldsymbol{u} - \frac{1}{2} \boldsymbol{M}^{-1} \begin{bmatrix} \boldsymbol{V}_q \\ \boldsymbol{V}_f \end{bmatrix}^T \left(\boldsymbol{Q}_N^i - \left(\boldsymbol{Q}_N^i \right)^T + \boldsymbol{B}_N^i \right) \boldsymbol{u}_N,$$

where $\boldsymbol{e}$ is a polynomial of degree N. If Assumption 1 is satisfied and $u(\boldsymbol{x})$ is polynomial, then the values of $u(\boldsymbol{x})$ at quadrature points are $\boldsymbol{u}_q = \boldsymbol{V}_q \boldsymbol{u}$ and $\boldsymbol{u} = \boldsymbol{P}_q \boldsymbol{u}_q$. This implies that $\boldsymbol{u}_f = \boldsymbol{V}_f \boldsymbol{P}_q \boldsymbol{u}_q = \boldsymbol{E} \boldsymbol{u}_q$. Expanding the latter term yields

$$\frac{1}{2} \boldsymbol{M}^{-1} \begin{bmatrix} \boldsymbol{V}_q \\ \boldsymbol{V}_f \end{bmatrix}^T \left(\boldsymbol{Q}_N^i - \left(\boldsymbol{Q}_N^i \right)^T + \boldsymbol{B}_N^i \right) \boldsymbol{u}_N$$

$$= \frac{1}{2} \boldsymbol{M}^{-1} \begin{bmatrix} \boldsymbol{V}_q \\ \boldsymbol{V}_f \end{bmatrix}^T \begin{bmatrix} \boldsymbol{Q}^i - \left(\boldsymbol{Q}^i \right)^T & \boldsymbol{E}^T \boldsymbol{B}^i \\ -\boldsymbol{B}^i \boldsymbol{E} & \boldsymbol{B}^i \end{bmatrix} \begin{bmatrix} \boldsymbol{u}_q \\ \boldsymbol{u}_f \end{bmatrix}$$

$$= \frac{1}{2} \boldsymbol{M}^{-1} \begin{bmatrix} \boldsymbol{V}_q \\ \boldsymbol{V}_f \end{bmatrix}^T \begin{bmatrix} \boldsymbol{Q}^i \boldsymbol{u}_q + \left(\boldsymbol{E}^T \boldsymbol{B}^i \boldsymbol{E} - \left(\boldsymbol{Q}^i \right)^T \right) \boldsymbol{u}_q \\ \boldsymbol{B}^i \left(\boldsymbol{u}_f - \boldsymbol{E} \boldsymbol{u}_q \right) \end{bmatrix}$$

$$= \frac{1}{2} \boldsymbol{M}^{-1} \boldsymbol{V}_q^T \left(\boldsymbol{Q}^i \boldsymbol{u}_q + \left(\boldsymbol{E}^T \boldsymbol{B}^i \boldsymbol{E} - \left(\boldsymbol{Q}^i \right)^T \right) \boldsymbol{u}_q \right).$$

Since $\boldsymbol{Q}^i = \boldsymbol{W} \boldsymbol{V}_q \boldsymbol{D}^i \boldsymbol{P}_q$ and $\boldsymbol{M} = \boldsymbol{V}_q^T \boldsymbol{W} \boldsymbol{V}_q$, we have that $\boldsymbol{M}^{-1} \boldsymbol{V}_q^T \boldsymbol{Q}^i \boldsymbol{u}_q = \boldsymbol{D}^i \boldsymbol{u}$. This simplifies the expression for error to

$$\boldsymbol{e}^T \boldsymbol{M} \boldsymbol{e} = \frac{1}{2} \boldsymbol{e}_q^T \left(-\boldsymbol{Q}^i \boldsymbol{u}_q + \left(\boldsymbol{E}^T \boldsymbol{B}^i \boldsymbol{E} - \left(\boldsymbol{Q}^i \right)^T \right) \boldsymbol{u}_q \right) \tag{30}$$

$$= -\frac{1}{2} \boldsymbol{e}_q^T \boldsymbol{Q}^i \boldsymbol{u}_q + \frac{1}{2} \boldsymbol{e}_q^T \left(\boldsymbol{E}^T \boldsymbol{B}^i \boldsymbol{E} - \left(\boldsymbol{Q}^i \right)^T \right) \boldsymbol{u}_q, \qquad \boldsymbol{e}_q = \boldsymbol{V}_q \boldsymbol{e}.$$

The remainder of the proof is similar to the proof of Lemma 1. Since $u \in P^M$ and $e \in P^N$, by exactness of the quadrature rules,

$$\boldsymbol{e}_q^T \left(\boldsymbol{E}^T \boldsymbol{B}^i \boldsymbol{E} - \left(\boldsymbol{Q}^i \right)^T \right) \boldsymbol{u}_q = \int_{\partial \widehat{D}} u e n_i - \int_{\widehat{D}} u \frac{\partial e}{\partial x_i} = \int_{\widehat{D}} \frac{\partial u}{\partial x_i} e = \boldsymbol{e}_q^T \boldsymbol{Q}^i \boldsymbol{u}_q.$$

Combining this with (30) implies that $\boldsymbol{e}^T \boldsymbol{M} \boldsymbol{e} = 0$, and since $\boldsymbol{M}$ is symmetric positive definite, $\boldsymbol{e} = 0$.

Lemma 8 suggests that, when a generalized SBP property does not hold, the use of under-integrated quadratures results in a loss of one or more orders of accuracy. For example, using $(N + 1)$ point GLL rules (which are exact for only polynomials of degree $2N - 1$) for either volume or surface quadratures should result in a loss of one order of accuracy compared to the use of $(N + 1)$-point Gauss rules (which are exact for polynomials of degree $2N$). This is indeed observed in numerical experiments.

8 Numerical experiments

In this section, we present two-dimensional experiments which verify the theoretical results presented and qualify the accuracy of the proposed methods. We begin by investigating the maximum stable timestep, stability, and accuracy of the skew-symmetric formulation on triangular and quadrilateral meshes, and conclude with two-dimensional experiments on a hybrid mesh containing mixed quadrilateral and triangular elements.

We consider numerical solutions of the 2D compressible Euler equations

$$\frac{\partial \rho}{\partial t} + \frac{\partial \left(\rho u\right)}{\partial x_1} + \frac{\partial \left(\rho v\right)}{\partial x_2} = 0,$$

$$\frac{\partial \rho u}{\partial t} + \frac{\partial \left(\rho u^2 + p\right)}{\partial x_1} + \frac{\partial \left(\rho uv\right)}{\partial x_2} = 0,$$

$$\frac{\partial \rho v}{\partial t} + \frac{\partial \left(\rho uv\right)}{\partial x_1} + \frac{\partial \left(\rho v^2 + p\right)}{\partial x_2} = 0,$$

$$\frac{\partial E}{\partial t} + \frac{\partial \left(u(E + p)\right)}{\partial x_1} + \frac{\partial \left(v(E + p)\right)}{\partial x_2} = 0,$$

where we have introduced the pressure is $p = (\gamma - 1)\left(E - \frac{1}{2}\rho(u^2 + v^2)\right)$ and the specific internal energy $\rho e = E - \frac{1}{2}\rho(u^2 + v^2)$.

We seek entropy stability with respect to the entropy for the compressible Navier-Stokes equations [18]

$$U(\boldsymbol{u}) = -\frac{\rho s}{\gamma - 1},$$

where $s = \log\left(\frac{p}{\rho^\gamma}\right)$ denotes the specific entropy. The mappings between conservative and entropy variables in two dimensions are given by

$$v_1 = \frac{\rho e(\gamma + 1 - s) - E}{\rho e}, \qquad v_2 = \frac{\rho u}{\rho e}, \qquad v_3 = \frac{\rho v}{\rho e}, \qquad v_4 = -\frac{\rho}{\rho e}$$

$$\rho = -(\rho e)v_4, \qquad \rho u = (\rho e)v_2, \qquad \rho v = (\rho e)v_3, \qquad E = (\rho e)\left(1 - \frac{v_2^2 + v_3^2}{2v_4}\right),$$

where ρe and s can be expressed in terms of the entropy variables as

$$\rho e = \left(\frac{(\gamma - 1)}{(-v_4)^\gamma}\right)^{1/(\gamma-1)} e^{\frac{-s}{\gamma-1}}, \qquad s = \gamma - v_1 + \frac{v_2^2 + v_3^2}{2v_4}.$$

There exist several choices for entropy conservative fluxes [37–39]. We utilize the the entropy conservative numerical fluxes given by Chandrashekar in [39]

$$f_{1,S}^1(\boldsymbol{u}_L, \boldsymbol{u}_R) = \{\!\{\rho\}\!\}^{\log}\{\!\{u\}\!\}, \qquad f_{2,S}^1(\boldsymbol{u}_L, \boldsymbol{u}_R) = \{\!\{\rho\}\!\}^{\log}\{\!\{v\}\!\},$$

$$f_{1,S}^2(\boldsymbol{u}_L, \boldsymbol{u}_R) = f_{1,S}^1\{\!\{u\}\!\} + p_{\text{avg}}, \qquad f_{2,S}^2(\boldsymbol{u}_L, \boldsymbol{u}_R) = f_{2,S}^1\{\!\{u\}\!\},$$

$$f_{1,S}^3(\boldsymbol{u}_L, \boldsymbol{u}_R) = f_{2,S}^2, \qquad f_{2,S}^3(\boldsymbol{u}_L, \boldsymbol{u}_R) = f_{2,S}^1\{\!\{v\}\!\} + p_{\text{avg}},$$

$$f_{1,S}^4(\boldsymbol{u}_L, \boldsymbol{u}_R) = (E_{\text{avg}} + p_{\text{avg}})\{\!\{u\}\!\}, \qquad f_{2,S}^4(\boldsymbol{u}_L, \boldsymbol{u}_R) = (E_{\text{avg}} + p_{\text{avg}})\{\!\{v\}\!\},$$

where the quantities $p_{\mathrm{avg}}, E_{\mathrm{avg}}, \|\boldsymbol{u}\|_{\mathrm{avg}}^2$ are defined as

$$p_{\mathrm{avg}} = \frac{\{\!\{\rho\}\!\}}{2\{\!\{\beta\}\!\}}, \qquad E_{\mathrm{avg}} = \frac{\{\!\{\rho\}\!\}^{\log}}{2\{\!\{\beta\}\!\}^{\log}(\gamma-1)} + \frac{\|\boldsymbol{u}\|_{\mathrm{avg}}^2}{2}, \qquad \beta = \frac{\rho}{2p},$$

$$\|\boldsymbol{u}\|_{\mathrm{avg}}^2 = 2(\{\!\{u\}\!\}^2 + \{\!\{v\}\!\}^2) - \left(\left\{\!\{u^2\}\!\right\} + \left\{\!\{v^2\}\!\right\}\right).$$

From here on, *entropy conservative* refers to a scheme which uses these entropy conservative fluxes at inter-element interfaces. We will refer to schemes which add interface dissipation as *entropy stable*. In this work, we utilize a local Lax-Friedrichs interface dissipation.

For all convergence experiments, we compare the numerical solution to analytic solution for the isentropic vortex problem [40]

$$\rho(\boldsymbol{x},t) = \left(1 - \frac{\frac{1}{2}(\gamma-1)(\beta e^{1-r(\boldsymbol{x},t)^2})^2}{8\gamma\pi^2}\right)^{\frac{1}{\gamma-1}}, \qquad p = \rho^\gamma,$$

$$u(\boldsymbol{x},t) = 1 - \frac{\beta}{2\pi}e^{1-r(\boldsymbol{x},t)^2}(x_2 - c_2), \qquad v(\boldsymbol{x},t) = \frac{\beta}{2\pi}e^{1-r(\boldsymbol{x},t)^2}(x_2 - c_2).$$

Here, u, v are the x_1 and x_2 velocity and $r(\boldsymbol{x},t) = \sqrt{(x_1 - c_1 - t)^2 + (x_2 - c_2)^2}$. The following experiments utilize $c_1 = 5, c_2 = 0$ and $\beta = 5$.

A low storage 4th order Runge-Kutta scheme [41] is used for all numerical experiments. The time-step is estimated based on formulas derived for linear advection in [22, 42]

$$dt = C\frac{h}{c_{\max}\max\left\{\frac{1}{2}C_T, C_I\right\}}$$

where h is the mesh size, $c_{\max}$ is the maximum wave-speed, C is a user-defined CFL constant, and C_T, C_I are constants in finite element inverse and trace inequalities. These constants scale proportionally to N^2, though precise values of C_I, C_T vary slightly depending on the choice of volume or surface quadrature used. The dependence of C_I, C_T on quadrature is discussed in more detail in Appendix A, where computed values of C_I, C_T are also given.

8.1 Choices of volume and surface quadrature considered

On quadrilaterals, we consider volume quadratures which are tensor products of one-dimensional quadrature rules, while for triangles we utilize volume quadratures from [25]. Surface quadratures are constructed face-by-face, and we refer to surface quadrature rules by the specific quadrature used over each face.

We consider three choices of volume and surface quadrature on quadrilaterals:

1. $(N+1)$ point GLL volume quadrature, $(N+1)$ point GLL surface quadrature.
2. $(N+1)$ point GLL volume quadrature, $(N+1)$ point Gauss surface quadrature,
3. $(N+1)$ point Gauss quadrature, $(N+1)$ point Gauss surface quadrature,

On triangles, we consider two cases:

1. degree $2N$ volume quadrature, $(N+1)$ point Gauss surface quadrature,
2. degree $2N$ volume quadrature, $(N+1)$ point GLL surface quadrature.

These choices can be combined to provide three different options on two-dimensional hybrid meshes of quadrilateral and triangular elements, which are motivated by balancing computational efficiency and accuracy:

1. Option 1: $(N+1)$ point GLL volume quadrature on quadrilaterals and $(N+1)$ point GLL surface quadrature on quadrilaterals and triangles.
2. Option 2: $(N+1)$ point GLL volume quadrature on quadrilaterals and $(N+1)$ point Gauss surface quadrature on quadrilaterals and triangles.
3. Option 3: $(N+1)$ point Gauss volume quadrature on quadrilaterals and $(N+1)$ point Gauss surface quadrature on quadrilaterals and triangles.

All three options assume a triangular volume quadrature which is exact for all polynomials of degree $2N$ or less.

All three options result in similar computational costs on on triangles, but slight differences in computational cost and complexity on quadrilaterals. On quadrilaterals, Option 1 is the most computationally efficient option, as the formulation (4) reduces to a standard entropy stable DG-SEM [11] or spectral collocation method [3]. Option 3 is most involved, resulting in a Gauss collocation method on quadrilaterals [5], and requires interpolation and two-point flux interactions between lines of volume quadrature nodes and boundary nodes.

Option 2 is slightly more expensive than Option 1, as the solution must be interpolated from GLL to Gauss nodes on the boundary. However, this is less expensive than Option 3 since volume GLL nodes include GLL boundary nodes as a subset. This implies that the matrix $\boldsymbol{V}_f$ is sparse, such that interpolation to boundary Gauss nodes involves only nodal values at boundary GLL nodes. Thus, Option 2 requires only two-point flux computations between boundary GLL and Gauss nodes. In contrast, the Gauss collocation scheme in Option 3 computes two-point flux interactions through $\boldsymbol{f}_S$ between each boundary node and a line of volume nodes.

8.2 Verification of discrete entropy conservation

We first verify that, for an entropy conservative flux and periodic domain, the spatial formulation tested against the projected entropy variables (15) is numerically zero. We refer to this quantity as the entropy right-hand side (RHS). Section 7.1 outlines conditions on quadrature accuracy which guarantee that the formulations (12) and (24) are discretely entropy conservative. These numerical results confirm that these conditions are tight.

We induce a curved polynomial mapping by defining curved coordinates $\widetilde{\boldsymbol{x}}$ through a mapping of Cartesian coordinates $\boldsymbol{x} \in [-1, 1]^2$

$$\widetilde{x}_1 = x_1 + \alpha \cos\left(\frac{\pi}{2} x_1\right) \sin\left(\pi x_2\right)$$
$$\widetilde{x}_2 = x_2 + \alpha \sin\left(\pi x_1\right) \cos\left(\frac{\pi}{2} x_2\right),$$

where $\alpha = 1/8$ for the following experiments. We vary the geometric degree of this mapping from $N_{\mathrm{geo}} = 1$ to $N_{\mathrm{geo}} = N$, where N_{geo} denotes the polynomial degree of the geometric mapping on a quadrilateral or triangular element.

Since Assumption 1 requires that the volume quadrature is sufficiently accurate to ensure that the mass matrix is positive-definite, we fix the volume to quadrature

	$N_{\text{geo}} = 1$	$N_{\text{geo}} = 2$	$N_{\text{geo}} = 3$	$N_{\text{geo}} = 4$	$N_{\text{geo}} = 5$	$N_{\text{geo}} = 6$
$M = 5$	8.68e-14	9.41e-14	9.31e-14	9.10e-14	9.92e-14	8.90e-14
$M = 3$	1.01e-13	8.87e-14	8.79e-14	9.68e-14	0.00833	0.00967
$M = 1$	1.8e-13	1.82e-13	1.998	2.104	2.080	2.086

(a) Triangular mesh

	$N_{\text{geo}} = 1$	$N_{\text{geo}} = 2$	$N_{\text{geo}} = 3$	$N_{\text{geo}} = 4$	$N_{\text{geo}} = 5$	$N_{\text{geo}} = 6$
$M = 5$	1.74e-14	1.06e-14	1.31e-14	1.35e-14	1.06e-14	1.31e-14
$M = 3$	2.89e-14	2.59e-14	2.83e-14	2.43e-14	3.20e-05	3.27e-05
$M = 1$	4.68e-14	3.77e-14	0.1548	0.1532	0.1517	0.1517

(b) Quadrilateral mesh

Table 1: Maximum absolute value of the entropy RHS over $t \in [0, 1]$ for degree $N = 6$ approximations on triangular and quadrilateral meshes. The volume quadrature for the quadrilateral mesh is taken to be $(N + 1)$-point GLL quadrature. The surface quadrature is taken to be a 1D GLL quadrature with a varying number of points, such that the rule is exact for degree $M + N$ polynomials.

to be exact for degree $2N$ polynomials on triangles. On quadrilaterals, we fix the volume quadrature to be an $(N+1)$ point GLL quadrature. To verify the conditions given in Section 7.1, we vary the accuracy of the 2D surface quadrature rule.

The initial condition is taken as the L^2 projection of the discontinuous profile

$$\rho = \begin{cases} 3 & |x - x_0| < 2.5 \\ 2 & \text{otherwise} \end{cases}, \qquad x_0 = 7.5, \qquad u = v = 0, \qquad p = \rho^\gamma.$$

We evolve the solution until final time $T = 1.0$ on a domain $[0, 15] \times [-.5, .5]$ using the skew symmetric formulation with $N = 6$ and a CFL of $1/2$. Table 1 shows the maximum entropy RHS over the duration of the simulation. We observe that for all $N_{\text{geo}} \leq M + 1$, the maximum entropy RHS is $O(10^{-14})$ and at the level of machine precision. When $N_{\text{geo}} > M + 1$, we observe that the maximum entropy RHS increases . We note that the case of $M = 5$ for the quadrilateral corresponds to the use of an $(N+1)$-point GLL rule for both volume and surface quadrature. The strong SBP property holds for this choice of quadrature, and the skew-symmetric formulation is equivalent to the entropy stable spectral collocation or DG-SEM methods of [3, 11].

8.3 Hybrid quadrilateral-triangular meshes

We conclude with experiments on a mixed mesh containing both quadrilateral and triangular elements (Figure 3a). Figure 3 shows L^2 errors for the isentropic vortex computed at $T = 5$ for Options 1, 2, and 3.

We observe that, in all cases, Option 1 is less accurate than Options 2 and 3, and that Option 3 achieves a rate of convergence close to the optimal $O(h^{N+1})$ rate, while Option 1 typically achieves rates of convergence between $O(h^N)$ and $O(h^{N+1/2})$. However, Option 2 behaves differently depending on the order N. For $N = 1$, Option 2 achieves an accuracy similar to Option 1. However, as N increases, Option 2 becomes more accurate. For $N = 4$, Option 2 achieves the same level of
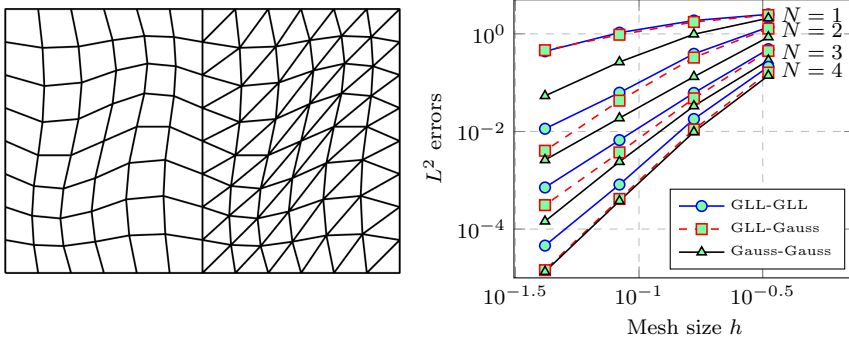
(b) Convergence for $N = 1, 2, 3, 4$

Fig. 3: Coarse hybrid mesh and L^2 errors for the isentropic vortex solution for Option 1, Option 2, and Option 3 for $N = 1, \ldots, 4$.

error observed for Option 3. This suggests that Lemma 8 may be sufficient but not necessary for full order accuracy.

9 Conclusions

We have constructed skew-symmetric "modal" DG formulations of nonlinear conservation laws which are entropy stable under less restrictive conditions on quadrature accuracy. These formulations are motivated by volume and surface quadratures which arise naturally on hybrid meshes. Because these quadrature rules do not necessarily induce operators which satisfy a "strong" matrix summation-by-parts property, we generalize proofs of entropy stability and free stream (constant) preservation using a weaker "variational" SBP property. This variational SBP property is also used to construct explicit conditions relating between the order of accuracy and degree of accuracy of each quadrature rule. Finally, we derive conditions between the degree of quadrature accuracy and polynomial degree of the geometric mapping under which the skew-symmetric formulation is entropy stable on curved meshes. Numerical experiments confirm the entropy stability and high order accuracy of the proposed schemes on triangular, quadrilateral, and 2D hybrid meshes.

10 Acknowledgments

N	1	2	3	4	5	6	7
Volume GLL	2	12	37.16	91.67	195.98	374.78	657.28
Volume Gauss	6	30	85.06	190.12	369.45	652.30	1072.75

(a) C_I, quadrilateral elements

N	1	2	3	4	5	6	7
Volume GLL, surface GLL	2	6	12	20	30	42	56
Volume Gauss, surface Gauss	6	12	20	30	42	56	72

(b) C_T, quadrilateral elements

N	1	2	3	4	5	6	7
Deg. $2N$ vol. quad. [25]	9	39.27	100.10	213.28	401.16	695.48	1127.48

(c) C_I, triangular elements

N	1	2	3	4	5	6	7
Surface GLL	12	16.14	20.52	28.12	35.42	45.97	55.76
Surface Gauss	6	10.90	16.29	24	31.88	42.42	52.89

(d) C_T, triangular elements

Table 2: Inverse and trace constants for triangular and quadrilateral elements with different quadrature configurations.

A Dependence of inverse and trace constants on quadrature

The maximum stable timestep under explicit time-stepping depends on specific choices of volume and surface quadrature. The dependence of timestep on quadrature has been documented for tensor product elements in [43], where they showed that for a high order Taylor method in time, the maximum stable timestep under $(N+1)$-point GLL volume and surface quadratures is roughly twice as large as the maximum stable timestep when volume/surface integrals are approximated using $(N + 1)$ point Gauss quadratures.

This discrepancy can be understood in terms of constants in finite element inverse and trace inequalities. It was shown in [22, 42] that, for linear problems, the maximum stable time-step scales inversely with the order-dependent constants C_I, C_T, where

$$\int_{\widehat{D}} |\nabla u|^2 \le C_I \int_{\widehat{D}} u^2, \qquad \int_{\partial \widehat{D}} u^2 \le C_T \int_{\widehat{D}} u^2, \qquad \forall u \in V^N. \tag{31}$$

Here, the integrals over $\widehat{D}, \partial \widehat{D}$ are computed using the same volume and surface quadrature rules used for computations. These constants can be used to bound surface integrals which appear in DG formulations, which can in turn be used to construct bounds on the spectral radius of DG discretization matrices. The maximum stable timestep $dt_{\max}$ is thus inversely proportional to the inverse and trace constants

$$dt_{\max} \propto C_T^{-1}, C_I^{-1}$$

The constants C_I, C_T depend on the choices of volume and surface quadrature used to evaluate each of the integrals in (31). It is known that L^2 norm computed using GLL quadrature is weaker than the full L^2 norm [26, 44]. For the domain $\widehat{D} = [-1, 1]^d$ in d dimensions, it can be shown that

$$\int_{\widehat{D}} u^2 \le \int_{\widehat{D}, \text{GLL}} u^2 \le \left(2 + \frac{1}{N}\right)^{d/2} \int_{\widehat{D}} u^2 \qquad \forall u \in Q^N, \tag{32}$$

where the middle integral is under-integrated using GLL quadrature. In other words, the discrete L^2 norm induced using GLL quadrature is weaker than the L^2 norm induced by a more accurate quadrature rule, which will be reflected in the trace and inverse constants.

Table 2 shows trace and inverse constants for triangular and quadrilateral elements under several different configurations of quadrature. For quadrilateral elements at high orders, we observe that the degree N inverse constants C_I under Gauss quadrature are roughly as large as the degree $(N+1)$ inverse constants under (volume) GLL quadrature. The degree N trace constants C_T under Gauss quadrature are exactly equal to the degree $(N+1)$ trace constants under GLL quadrature, which was proven in [22]. Trace constants under GLL volume and Gauss surface quadrature are also identical to trace constants computed using GLL quadrature for both volume and surface integrals, which is a consequence of the lower bound in (32).

Several observations can be made based on the values of C_I, C_T presented in Table 2. On quadrilaterals, the maximum stable time-step for a degree N DG scheme using Gauss quadrature is expected to be smaller than that of a degree N scheme using GLL quadrature, which matches observations in [43]. Additionally, the maximum stable timestep under GLL volume quadrature and Gauss surface quadrature should be the same as the maximum stable timestep when GLL quadrature is used for both volume and surface integrals (e.g. DG-SEM). For triangles, the maximum stable timestep should be smaller under surface GLL quadrature compared to surface Gauss quadrature. However, we note that, while bounds on the maximum stable time-step can be derived based on the constants C_I, C_T [22, 42], these bounds are not tight for upwind or dissipative fluxes [45].

References

 1. Gregor J Gassner. A skew-symmetric discontinuous Galerkin spectral element discretization and its relation to SBP-SAT finite difference methods. *SIAM Journal on Scientific Computing*, 35(3):A1233–A1253, 2013.
 2. Travis C Fisher and Mark H Carpenter. High-order entropy stable finite difference schemes for nonlinear conservation laws: Finite domains. *Journal of Computational Physics*, 252:518–557, 2013.
 3. Mark H Carpenter, Travis C Fisher, Eric J Nielsen, and Steven H Frankel. Entropy Stable Spectral Collocation Schemes for the Navier–Stokes Equations: Discontinuous Interfaces. *SIAM Journal on Scientific Computing*, 36(5):B835–B867, 2014.
 4. Jared Crean, Jason E Hicken, David C Del Rey Fernández, David W Zingg, and Mark H Carpenter. Entropy-stable summation-by-parts discretization of the Euler equations on general curved elements. *Journal of Computational Physics*, 356:410–438, 2018.
 5. Jesse Chan, David C Fernandez, and Mark H Carpenter. Efficient entropy stable Gauss collocation methods. *arXiv preprint arXiv:1809.01178*, 2018.
 6. Jesse Chan. On discretely entropy conservative and entropy stable discontinuous Galerkin methods. *Journal of Computational Physics*, 362:346 – 374, 2018.
 7. Jesse Chan and Lucas C Wilcox. Discretely entropy stable weight-adjusted discontinuous Galerkin methods on curvilinear meshes. *arXiv preprint arXiv:1805.10934*, 2018.
 8. Zhijian J Wang, Krzysztof Fidkowski, Rémi Abgrall, Francesco Bassi, Doru Caraeni, Andrew Cary, Herman Deconinck, Ralf Hartmann, Koen Hillewaert, Hung T Huynh, et al. High-order CFD methods: current status and perspective. *International Journal for Numerical Methods in Fluids*, 72(8):811–845, 2013.
 9. Mark Ainsworth. Dispersive and dissipative behaviour of high order discontinuous Galerkin finite element methods. *Journal of Computational Physics*, 198(1):106–130, 2004.
10. Miguel R Visbal and Datta V Gaitonde. High-order-accurate methods for complex unsteady subsonic flows. *AIAA journal*, 37(10):1231–1239, 1999.
11. Gregor J Gassner, Andrew R Winters, and David A Kopriva. Split form nodal discontinuous Galerkin schemes with summation-by-parts property for the compressible Euler equations. *Journal of Computational Physics*, 327:39–66, 2016.
12. Gregor J Gassner, Andrew R Winters, Florian J Hindenlang, and David A Kopriva. The BR1 scheme is stable for the compressible Navier–Stokes equations. *Journal of Scientific Computing*, pages 1–47, 2017.
13. Jared Crean, Jason E Hicken, David C Del Rey Fernández, David W Zingg, and Mark H Carpenter. High-Order, Entropy-Stable Discretizations of the Euler Equations for Complex Geometries. In *23rd AIAA Computational Fluid Dynamics Conference*. American Institute of Aeronautics and Astronautics, 2017.
14. Tianheng Chen and Chi-Wang Shu. Entropy stable high order discontinuous Galerkin methods with suitable quadrature rules for hyperbolic conservation laws. *Journal of Computational Physics*, 345:427–461, 2017.

15. Matteo Parsani, Mark H Carpenter, Travis C Fisher, and Eric J Nielsen. Entropy Stable Staggered Grid Discontinuous Spectral Collocation Methods of any Order for the Compressible Navier–Stokes Equations. *SIAM Journal on Scientific Computing*, 38(5):A3129–A3162, 2016.
16. Lucas Friedrich, Andrew R Winters, David C Fernández, Gregor J Gassner, Matteo Parsani, and Mark H Carpenter. An Entropy Stable h/p Non-Conforming Discontinuous Galerkin Method with the Summation-by-Parts Property. *arXiv preprint arXiv:1712.10234*, 2017.
17. Jason E Hicken, David C Del Rey Fernández, and David W Zingg. Multidimensional summation-by-parts operators: General theory and application to simplex elements. *SIAM Journal on Scientific Computing*, 38(4):A1935–A1958, 2016.
18. Thomas JR Hughes, LP Franca, and M Mallet. A new finite element formulation for computational fluid dynamics: I. Symmetric forms of the compressible Euler and Navier-Stokes equations and the second law of thermodynamics. *Computer Methods in Applied Mechanics and Engineering*, 54(2):223–234, 1986.
19. Michael S Mock. Systems of conservation laws of mixed type. *Journal of Differential equations*, 37(1):70–88, 1980.
20. Amiram Harten. On the symmetric form of systems of conservation laws with entropy. *Journal of computational physics*, 49(1):151–164, 1983.
21. Constantine M Dafermos. *Hyperbolic conservation laws in continuum physics*. Springer, 2005.
22. Jesse Chan, Zheng Wang, Axel Modave, Jean-Francois Remacle, and T Warburton. GPU-accelerated discontinuous Galerkin methods on hybrid meshes. *Journal of Computational Physics*, 318:142–168, 2016.
23. David C Del Rey Fernández, Pieter D Boom, and David W Zingg. A generalized framework for nodal first derivative summation-by-parts operators. *Journal of Computational Physics*, 266:214–239, 2014.
24. Hendrik Ranocha. Generalised summation-by-parts operators and variable coefficients. *Journal of Computational Physics*, 362:20 – 48, 2018.
25. H Xiao and Zydrunas Gimbutas. A numerical algorithm for the construction of efficient quadrature rules in two and higher dimensions. *Comput. Math. Appl.*, 59:663–676, 2010.
26. Claudio Canuto, M Yousuff Hussaini, Alfio Quarteroni, and Thomas A Zang. *Spectral Methods: Fundamentals in Single Domains*. Springer Science & Business Media, 2007.
27. Eitan Tadmor. The numerical viscosity of entropy stable schemes for systems of conservation laws. I. *Mathematics of Computation*, 49(179):91–103, 1987.
28. Cengke Shi and Chi-Wang Shu. On local conservation of numerical methods for conservation laws. *Computers and Fluids*, 2017.
29. PD Thomas and CK Lombard. Geometric conservation law and its application to flow computations on moving grids. *AIAA journal*, 17(10):1030–1037, 1979.
30. David A Kopriva. Metric identities and the discontinuous spectral element method on curvilinear meshes. *Journal of Scientific Computing*, 26(3):301–327, 2006.
31. Miguel R Visbal and Datta V Gaitonde. On the use of higher-order finite-difference schemes on curvilinear and deforming meshes. *Journal of Computational Physics*, 181(1):155–185, 2002.
32. Florian Hindenlang, Gregor J Gassner, Christoph Altmann, Andrea Beck, Marc Staudenmaier, and Claus-Dieter Munz. Explicit discontinuous Galerkin methods for unsteady problems. *Computers & Fluids*, 61:86–93, 2012.
33. Jan S Hesthaven. From electrostatics to almost optimal nodal sets for polynomial interpolation in a simplex. *SIAM Journal on Numerical Analysis*, 35(2):655–676, 1998.
34. T Warburton. An explicit construction of interpolation nodes on the simplex. *Journal of engineering mathematics*, 56(3):247–262, 2006.
35. Jesse Chan and T Warburton. A comparison of high order interpolation nodes for the pyramid. *SIAM Journal on Scientific Computing*, 37(5):A2151–A2170, 2015.
36. Andrew R Winters, Dominik Derigs, Gregor J Gassner, and Stefanie Walch. A uniquely defined entropy stable matrix dissipation operator for high Mach number ideal MHD and compressible Euler simulations. *Journal of Computational Physics*, 332:274–289, 2017.
37. Farzad Ismail and Philip L Roe. Affordable, entropy-consistent Euler flux functions II: Entropy production at shocks. *Journal of Computational Physics*, 228(15):5410–5436, 2009.
38. Hendrik Ranocha. Comparison of some entropy conservative numerical fluxes for the Euler equations. *Journal of Scientific Computing*, 76(1):216–242, 2018.

39. Praveen Chandrashekar. Kinetic energy preserving and entropy stable finite volume schemes for compressible Euler and Navier-Stokes equations. *Communications in Computational Physics*, 14(5):1252–1286, 2013.
40. Chi-Wang Shu. Essentially non-oscillatory and weighted essentially non-oscillatory schemes for hyperbolic conservation laws. In *Advanced numerical approximation of nonlinear hyperbolic equations*, pages 325–432. Springer, 1998.
41. Mark H Carpenter and Christopher A Kennedy. Fourth-order $2n$-storage Runge-Kutta schemes. Technical Report NASA-TM-109112, NAS 1.15:109112, NASA Langley Research Center, 1994.
42. Jesse Chan and John A Evans. Multi-patch discontinuous Galerkin isogeometric analysis for wave propagation: Explicit time-stepping and efficient mass matrix inversion. *Computer Methods in Applied Mechanics and Engineering*, 333:22–54, 2018.
43. Gregor Gassner and David A Kopriva. A comparison of the dispersion and dissipation errors of Gauss and Gauss–Lobatto discontinuous Galerkin spectral element methods. *SIAM Journal on Scientific Computing*, 33(5):2560–2579, 2011.
44. Alfio Quarteroni and Alberto Valli. *Numerical Approximation of Partial Differential Equations*. Springer, 1994.
45. Lilia Krivodonova and Ruibin Qin. An analysis of the spectrum of the discontinuous Galerkin method. *Applied Numerical Mathematics*, 64:1–18, 2013.